THE LATERAL INSTABILITY OF A SIMPLY SUPPORTED DEEP BEAM SUBJECTED TO A CONCENTRATED LOAD AT ITS CENTROID

A THESIS

SUBMITTED TO THE DEPARTMENT OF AERONAUTICS AND ASTRONAUTICS

AND THE COMMITTEE ON THE GRADUATE DIVISION

OF STANFORD UNIVERSITY

IN PARTIAL FULFILLMENT OF THE REQUIREMENTS

FOR THE DEGREE OF

ENGINEER

by

LCDR Edward R. Way, USN

May 1967

ACKNOWLEDGEMENT

The investigation of the lateral buckling of a simply supported deep beam was conducted as a portion of the general research of the behavior of structural members being performed by the Department of Aeronautics and Astronautics at Stanford University.

For the opportunity to pursue an advanced education, appreciation is hereby extended to the United States Navy and its Professional Development Program.

Principal acknowledgement is expressed to Professor Wilfred H. Horton, who initially conceived the research herein described, and whose advice, inspiration and assistance made possible the successful completion of this work.

TABLE OF CONTENTS

LIST OF TABLES

LIST OF TABLES (Cont.)

LIST OF FIGURES

LIST OF FIGURES (Cont.)

LIST OF FIGURES (Cont.)

LIST OF SYMBOLS

δ	lateral deflection
E	Young's Modulus
G	torsion modulus
I	moment of inertia
J	polar moment of inertia
k	spring constant of elastic restraint
L	length
P	applied load
P_{cr}	critical load
$P_{o_{cr}}$	critical load of deep beam with no elastic restraint at centroid
$\frac{\Delta x}{\Delta y}$	inverse slope of Southwell plot

I. INTRODUCTION

Although the theoretical solution to the problem of the lateral buckling of a simply supported deep beam subjected to a concentrated load at its centroid has existed for many years,[1,2] experimental investigation to substantiate the theory has not been entirely definitive. Bromley and Robinson,[3] in fact, were unable to achieve agreement between theory and experiment. Trayer and March[4] attempted to analyze this apparent discrepancy and obtained satisfactory agreement with theory in their own tests. Further experimental verification is shown in a paper by Dumont and Hill.[5]

In recent years Massey[6] showed that it is possible to determine the theoretical critical load for lateral buckling of an I beam by interpreting data obtained from tests on a realistic beam using a technique which results in a linear plot. He also showed that the method could be altered to include the deep beam. Although, strictly speaking, Massey's development did not produce a true Southwell plot as he indicated, a later study by Horton[7] reduced the mathematical analysis of the deep beam to one in which the Southwell technique was applicable.

Southwell[8] developed his basic theory in 1932 as a means of verifying the theory of buckling of perfect columns. The Southwell plot depends upon the fact that the deflection at an appropriate point can be expressed as the sum of a series of terms which are associated with the initial irregularities and the actual and critical loads for the structure. Under appropriate conditions,

that is, when the load on the structure approaches the theoretical critical value and the deflection is recorded at a point in which only one harmonic is significant, only the first term of the series is of importance. In these cases, the relationship between load and deflection approximates to a rectangular hyperbola. Southwell points out that by a simple change of variable this curve can be presented as a straight line, the inverse slope of which has a value equivalent to the classical critical load and that the intercept of the line with the appropriate axis is a measure of the initial imperfection.

The mathematical analysis which Southwell made was performed only for the simple column but a more general analysis made by Westergaard[9] gave clear indication of much wider applicability. This wider applicability is of greatest importance in studies of stability. In theory, buckling takes place when the deflection of the body increases indefinitely without further increase in load and, for an initially perfect specimen, no motion will occur until the critical load level is reached. In practice, however, neither of these conditions are met in real structures. Deformations occur from the very onset of loading and increase continuously with increasing load until collapse takes place. It is difficult from such load-displacement data to define a critical load and indeed it is often questionable as to whether or not such a value exists unless one becomes concerned with questions of inelastic behavior. Correlation between theory for the ideal body and actual experimental results can only be made on the basis of an implicit relationship such as that contained in the Southwell

formulation.

Just as a consideration of the behavior of a column with a small displacement analysis leads to the Southwell method of data reduction, so an examination of the elastica leads to a potential large displacement technique. It can be shown mathematically[10] that the equation of the elastica can be approximated very closely by a parabola and, as a consequence of this relationship, when the square of the deflection is plotted as a function of load, a linear relationship is obtained. This line intercepts the load axis at a point which is defined by the theoretical critical load value for the ideal column. There is much practical evidence to indicate that this large displacement law may be as general as that of Southwell. Queinec[11] has demonstrated its applicability in certain problems of buckling due to thermal stress and in researches made concurrently with those described here, Willey[12] successfully established its applicability to flat plates under uniform axial compression.

With this background in mind, the approach to the research that comprises this paper emerged. Initial experimentation with a simply supported Euler column was undertaken because complete theoretical analyses of all phases of the problem are available. Timoshenko[1] presents the classical buckling theory for the column. Southwell[8] and Horton[10] analytically justify, respectively, the small and large deflection determinations of critical load. Too, testing procedures for a simply supported Euler column are elementary, and this lends itself particularly well to the initial probe of a concept intended for expanded application in a more difficult

problem. Experimental correlation of the predicted buckling loads of the perfect column by these three independent means, therefore, would support the idea that a similar correlation might apply to the case of the lateral instability of the deep beam.

Given that the outcome of the tests on the column were favorable, the deep beam would be tested in a like manner. Southwell data would hopefully predict the critical load of the unrestrained beam and permit the determination of the stability boundary for the elastically restrained beam. These results could then be compared with available theoretical analyses. Large deflection measurements on the unrestrained beam would next answer the question of the validity of the hypothesis that large deflection data can be applied to the problem of lateral instability of the deep beam. With this approach in mind, the experimental work was begun.

II. DISCUSSION OF THE PROBLEM

A certain amount of experimental work has been done on the problem of the lateral buckling of deep beams.[3,4,5,6] The results obtained are, in general, rough verifications of the elementary case of first mode buckling of the simply supported beam. But the early studies of the 1930's[3,4,5] give no indication of the means by which buckling was defined. At the time these papers were published Southwell's work was new and all but unknown, and several diverse and unrelated ideas existed which supposedly enabled the experimenter to pinpoint the onset of buckle in a structure. The top of the knee method and the strain reversal method are good examples of two of the more widely accepted of these devices. However, these and other methods in use at the time give, at best, highly scattered results and in many instances can produce meaningless conclusions. Further, none of these ideas were ever substantiated by any legitimate theoretical development.

Massey's paper,[6] written in 1964, developed the use of a linear plot by which one could predict the lateral buckling loads of I beams and deep beams. This was a significant step forward because the approach introduced a consistency of results that was not possible with the earlier methods. But when Horton[7] was able to show analytically that the Southwell plot was applicable to the lateral instability of deep beams he introduced a device which, if it could be demonstrated experimentally, would not only predict the theoretical buckling load of a deep beam, but would have the added virtue of being a method already proven to be applicable to

a diversity of buckling problems. The efficacy of such a demonstration is clear in that it would lend further credence to the generality of the Southwell technique.

Establishing positive results for a simple problem as the basis for methods of solving more difficult cases has proven by experience to be a logical experimental approach. This concept was used to twofold advantage in the work that comprises this thesis. First, if complete correlation of analytic, Southwell and large deflection predictions of the buckling load could be established for an Euler column, where experimental procedures are quite simple, it would not be wholly unreasonable to expect a similar result for the deep beam. Second, by doing initial deep beam experiments on a specimen which was not elastically restrained, (essentially a repeat of work done by Massey[6]) the validity of application of the Southwell plot to this problem could be shown. This contribution would be significant since Massey's paper, in the strict sense, does not do this. By-products of such tests would also emerge. It could be determined what effect, if any, the process of repeated tests on a given specimen had upon the critical load prediction. Also, if meaningful results were to be obtained in later tests where elastic restraints were imposed, it was necessary to know that the apparatus used could give good accuracy in the simpler case of the unrestrained beam.

In devising a test rig for experiments on the deep beam, considerable care was necessary to avert foreseeable difficulties. If the beam were loaded, as shown in Ref. 13, in a standard hydraulic testing machine, side loads could develop which might in-

duce sizeable errors in any results obtained. By dead loading the beam this drawback was eliminated. The beam was made of sufficient length to avoid any problem involving transverse shear and construction of the end supports was done with great care because even small deviations from the simple support condition could introduce intolerable errors in the test results. Another source of possible error was eliminated by measuring deflections by optical means, forestalling any difficulty that would result from the use of contact measuring devices. Measurements of displacement at different points along the beam made it possible to determine what effect, if any, the location of measurement has upon the prediction of buckling load. Overlooking any of these factors could seriously affect the outcome of the test results and a dramatic demonstration of this statement is evident when a comparison is made between the predicted buckling loads that result from the deflection measurements at the centroid of the deep beam and those made at the quarter length points when an elastic restraint of large spring constant is imposed at the centroid.

III. EQUIPMENT

Three separate test rigs were used to perform the experiments that comprise the heart of this work. Fig. 1 is a sketch of the basic equipment used to acquire the data for the buckling of the Euler column. Figs. 3a through 5b depict the apparatus which yielded the bulk of data for the deep beam, restrained and unrestrained, in the small deflection region. And, in Figs. 7a through 7c, the equipment which produced the large deflection information on the deep beam is shown.

The first tests to be run were performed on an Euler column of dimensions 6.000 X 0.2754 X 0.01665 inches. The column was of steel and the ends were ground to knife edges to approximate the simple support condition. The essential element of the test rig, shown in Fig. 1, was a simple chemical balance which rested on the lower (fixed) loading head of a compression test machine. A measuring scale, consisting of a metal plate covered with graph paper graduated in millimeters, was attached to the upper (movable) head of the test machine and was used to read lateral deflections of the column under load. The column was magnetized so that it would cling to the upper loading head. By doing this the specimen was easily positioned and alignment was automatic because the column hung vertically under the force of gravity. Metric weights were then used to apply the load to the column through the mechanism of the chemical balance.

Small deflection measurements were next taken on a deep steel beam 30.69 inches long, 1.95 inches deep and 0.0591 inches

thick. Figs. 3a and 3b depict the overall arrangement of equipment.

The essential parts of the foundation upon which the beam was mounted were a pair of large steel blocks, the surfaces of which had been ground smooth to provide minimum rolling resistance to the end restraints of the beam which were to be placed upon the blocks. The optical collimator used for the measurement of deflections and the weight cage which constituted the method of load application are also apparent in these figures. The small hook on the bottom of the weight cage, visible in Fig. 3b, provided a means of continuous load application at any desired rate. A container was placed on the hook and water could then be piped into the container, the rate of flow of the water, of course, governing the loading rate.

Figs. 4a and 4b are close-up views of the apparatus. From Fig. 4a the method of measuring displacement is clear. Mounted upon the loading yoke is an ordinary six inch metal ruler, graduated in hundredths of an inch. As the load was applied, the beam deflected and, since the loading yoke was mounted at the centroid of the beam, a measurement of the deflection of this yoke was also a measurement of the motion of the centroid of the beam. By sighting through the collimator onto the ruler, it was possible to measure deflections to an accuracy of one or two thousandths of an inch.

The loading yoke is evident in Fig. 4b but it is much more clearly shown in Fig. 5b. It consisted merely of a prong shaped aluminum piece through which two holes were made. A pin inserted

through these holes passed also through a hole at the beam's centroid. At the base of the yoke a shaft was attached which extended to the load transducer, which can be seen most clearly in Fig. 4b. It is the ring shaped device at the center of the picture and upon this ring were mounted four strain gages. The gages were wired into a bridge and then connected to a Model 150-1100 Sanborn Carrier Amplifier and a Sanborn 151 Single Channel Recorder. The electronic equipment is not shown in the figures, however.

The method of supporting the ends of the beam can be seen in Figs. 4a, 4b and 5a. On each end of the beam were situated two aluminum blocks, held together by three bolts. On the inner side of each block, a groove was cut in the vertical direction and in each groove was fitted a steel rod of round cross section and of a length equal to the height of the blocks. The beam was placed so that it was restrained by the rods about one quarter of an inch from the end of the beam, the bolts were fastened so that they were finger tight and then the combination of blocks and beam were mounted on four more rods of round cross section, two at each end, as can be seen in Figs. 4a, 4b and 5a, which acted as rollers for the entire apparatus. A reasonably heavy weight was then placed on each end block. The result was a support which gave very little restraint to end motion of the beam in any form except that all tendency of the end to twist was restrained. The method gave a very close approximation to the simple support condition of the theoretical problem.

In Figs. 5a and 5b, the mechanism used to impose the elastic restraint at the beam center is visible. The restraint used

was a rigidly mounted cantilever spring, the length of which was made adjustable so that various spring values could be imposed. The spring can be seen, in Fig 5b, to be placed against the loading yoke. Since the yoke moves with the beam centroid, restricting yoke motion obviously restricts the motion of the center of the beam.

Not shown in the figures is the device used to measure deflections at the quarter length points of the beam. When such measurements were needed, depth micrometers were mounted at the appropriate locations, and adjusted as necessary to measure the desired displacements.

The equipment used in the large deflection measurements is depicted in Figs. 7a through 7c. The beam shown is of fibreglass but the same set-up was used when measuring the deflections of a similar beam made of spring steel. Both beams were 20.91 inches long and 1.50 inches in depth. The glass beam had a thickness of 0.0345 inches and the spring steel beam a thickness of 0.0148 inches. When a beam was to be tested, it was first clamped into end supports which are visible in Figs. 7b and 7c. The supports were round aluminum rods, slotted to receive the ends of the beam, and pointed at the lower ends to provide simple support conditions.

The entire large deflection apparatus was mounted on two heavy steel blocks, one at each end of the beam, the blocks providing the stationary foundation for the rest of the rig. Onto each large block were clamped two smaller steel blocks, positioned so that a space existed between them just large enough to allow free motion of the beam end supports. To reduce the frictional

resistance to end shortening of the beam as it was deformed, four roller bearings were inserted between each of the two pairs of small steel blocks, and then a plate was laid atop the roller bearings. Onto the plate, then, was placed the pointed end of the beam end support previously described. Measurements of deflection were made optically with the use of a ruler graduated in hundredths of an inch, but this is not shown in the figures.

This relatively crude device provided a rough approximation of a simple support and could allow considerable beam distortion. The motion of the end support in the gap between the small steel blocks, after friction had been overcome, was such that only twisting of the beam was prevented, and this approximated the theoretical simple support condition to an adequate degree of accuracy.

IV. TEST PROCEDURES

Preliminary experimentation began with tests on a steel column 6.000 X 0.02754 X 0.01665 inches in dimension and knife-edged at the ends to simulate simple supports. By suspending the column magnetically from the upper (movable) head of a test machine, shown in Fig. 1, and lowering the head until the lower end of the column just touched one of the tables of the chemical balance, proper positioning and alignment were assured. Metric weights were then added to the other table and, with each increment of weight, the upper head of the test machine was adjusted so that the deflection needle of the chemical balance was repositioned to zero. This procedure, of course, insured that the load on the column was exactly equivalent to the weights on the balance table. At each step, a record was made of the load on the column and its maximum lateral deflection. Seven tests were run and the data from the tests is recorded in Tables 1a and 1b. The data was then averaged in Table 1c and load-deflection, Southwell and large deflection plots were constructed from the averaged data. These plots are shown in Figs. 2a through 2c.

Small deflection theory for the deep beam was verified using the test equipment shown in Figs. 3a through 5b. A steel beam of dimensions 30.69 X 1.95 X 0.0591 inches was used and initial measurements were taken to check the theory for lateral buckling of the beam with no elastic restraint imposed. The load on the beam when the initial displacement reading was taken totaled 7.7 pounds. This initial load consisted of all the parts of the loading device;

the yoke, the load transducer, the cage on which the discrete weights were placed and the container used when the load was incremented by the use of running water.

In the case where the beam was buckled without an elastic restraint at the centroid, the loading method used was one utilizing running water. Load readings were determined by interpreting load cell readings on the Sanborn equipment. These loads were read at predetermined increments of displacement as measured by the optical collimator. A physical restriction was placed on the maximum deflection of the beam so that it would not exceed the elastic limit.

Ten initial tests were performed in the manner described, so that reliability of the experimental data might be evaluated by examining the repeatability of the experimental evaluation of critical load. The data from all ten tests was virtually identical and, therefore, only the data of the last two tests is presented. Tables 2a and 2b are the results of these two tests, while Fig. 8a is the resultant load versus displacement plot. Fig. 8b is the Southwell interpretation of the data and the consistency of the results is self evident.

After these initial tests, various elastic restraints were imposed at the centroid of the beam. Figs. 5a and 5b show the method of imposing the restraint. A steel cantilever spring of variable length was used to restrict the motion of the yoke and, since the yoke moved with the beam centroid, the centroid of the beam was thereby elastically restrained. The various spring values were experimentally determined by averaging a series of load-

deflection measurements at chosen increments of spring length.

The large initial load of 7.7 pounds, which was tolerated when the deep beam was tested without elastic restraint, introduced no essential difficulty. The collimator was zeroed with the initial load on the beam and readings commenced from this zero setting. All that was necessary to compensate the data for the initial load was to determine the displacement of the beam due to this load by extrapolation of the load-displacement curve through the first few loading points to the point of zero load. Then the initial displacement value was added to the displacement reading for each increment of load. But the size of the initial displacement due to a load of 7.7 pounds might have proved intolerable in the case of the elastically restrained beam because the beam would have been slightly distorted before the spring came in contact with the yoke. Thus, in order to approach zero deflection when the spring was initially placed in contact, the initial load had to be reduced. By removing all loading components except the yoke and load cell, the initial load was reduced to about 1.20 pounds, a force which caused a negligible initial deflection in the unrestrained beam. The spring was then moved toward the yoke until it barely made contact. Then the measurement system was zeroed and readings commenced.

It was discovered that, at low values of spring constant, measurements of motion of the centroid gave valid data with which to calculate critical buckling load. However, as the spring value increased, the motion of the centroid decreased and became difficult to measure. For these higher spring constants, measurements of

deflections at the quarter length points of the beam were made, in addition to measurements at the centroid, by the use of depth micrometers placed at the quarter points of the beam. Tables 3a through 3n and Figs. 9a through 9r provide a means of comparison of data resulting from the various points of measurement.

An attempt was made to obtain large deflection readings for the deep beam on which, to this point, only small deflection data had been compiled. However, because the steel of this beam was not of highest quality, it was found that the material entered the region of plastic deformation soon after the beam departed from the realm of small deflections. A fibreglass beam was tried and although some deceptively consistent data emerged from these tests, it was apparent that the non-linear characteristics of the fibreglass material caused the predicted critical loads from the large and small deflection data to differ widely.

A beam made of high quality spring steel was tested next and gave satisfactory results. The test procedure used was quite simple. Utilized was the test set-up shown in Figs. 7a through 7c. Discrete weight increments were applied to the beam centroid, and measurements of deflection were taken for each weight increment. It was discovered early in the tests of the glass beam that, whether the measurements of deflection were taken at the beam's centroid or at the top fibre, the critical load resulting from the data was the same, as can be seen from Figs. 10b and 10e and from Figs. 10c and 10f. This valuable information was used when testing the spring steel beam. Because it was much easier to do so, the displacements of this beam were measured at the center of the top fibre. The

data for the spring steel beam is presented in Table 5 and in Figs. 11a through 11c.

It should be mentioned that, because the large deflections of the fibreglass and spring steel beams induced considerable friction forces at the end supports, it became very difficult to determine the equilibrium position for each increment of load. The method used, as motions became increasingly restricted by friction, was to first load the beam, to then manually displace it to a state of deflection in excess of what would occur because of the load imposed on it, and finally, to manually vibrate the ends until the beam receded to an equilibrium position, as shown in Fig. 7c. Because the equilibrium position was not easily detectable, each test required between three and six hours to perform. For this reason, if further studies in the realm of large deflections of a deep beam are undertaken, it would be well to consider a more elaborate end support device, operating perhaps on ball bearings, so that end support friction can be made less of a problem. This one improvement would remove a great deal of tedium from the testing procedure.

V. DISCUSSION OF RESULTS

The theoretical critical load for a simply supported Euler column is given by the equation

$$P_{cr} = \frac{\pi^2 EI}{L^2} \qquad (1)$$

where

E = Young's Modulus for the material of the column (3×10^7 psi for steel in the case of the column tested)

I = moment of inertia about the axis of least bending resistance

L = length of the column.

The equation yields a theoretical buckling load of

$$P_{cr} = 0.8695 \text{ lb} = 395.0 \text{ gm}$$

for the column tested, which had dimensions of 6.000 X 0.01665 X 0.2754 inches.

From the data of Table 1c, which is the averaged data for the tests on the Euler column, Figs. 2a through 2c were drawn. The inverse slope of the curve of Fig. 2b, the Southwell plot of the small deflection data for the column, yields a critical load of 409 grams. The deviation of this value from theory is about 3.5%.

The large deflection plot of Fig. 2c provides an indication of critical load when the straight segment of the curve is extrapolated to the load axis, or, to the line of zero deflection. This curve gives a critical load value of 395.6 grams. The deviation from the Southwell determination is about 3.5% and from theory it is almost zero.

The result, then, is a simple experimental demonstration

that measurements in the pre- and post-buckled regions can be used to determine the critical load of a column. The Southwell and large deflection curves combine with the analytical solution to provide a three way verification of buckling load. Of prime importance now is whether the same results can be obtained in the case of the deep beam.

Timoshenko[1] develops the equation

$$P_{o_{cr}} = \frac{16.94\sqrt{EIGJ}}{L^2} \qquad (2)$$

which yields the first mode lateral buckling load of a simply supported deep beam of rectangular cross section when subjected to a concentrated load at the centroid. The terms of the equation are:

$P_{o_{cr}}$ = critical buckling load of beam in first mode
E = Young's Modulus of beam material
I = moment of inertia of beam cross section
G = torsion modulus of beam material
J = polar moment of inertia of the cross section
L = length of beam

By altering the development presented by Timoshenko so that it conforms to the second mode shape, equation (2) becomes

$$P_{cr} = \frac{44.5\sqrt{EIGJ}}{L^2}. \qquad (3)$$

The deep beam used in the small deflection research had dimensions of 30.69 X 1.95 X 0.0591 inches. The beam was of steel and the values for E and G were taken as 3×10^7 psi and 1.1×10^7 psi respectively. With these values, equation (2) produces a theoretical first mode buckling load of 22.0 pounds. Equation (3) yields 57.9 pounds as the second mode critical load.

If the Southwell approach is valid when applied to the lateral buckling of a deep beam, the inverse of the slope of the

Southwell plots for the first and second mode cases, that is the cases where the beam is without lateral restraint at the centroid and where the lateral restraint is infinitely stiff, should equal the theoretical buckling loads for these conditions.

Tables 3a and 3n and Figs. 9b and 9q show that the Southwell plots yield values of 21.4 pounds and 58.5 pounds for the first and second mode critical loads, respectively. The respective deviations from theory are 2.8 percent and 1.0 percent.

The addition of a finite elastic restraint at the centroid of the beam, so that the lateral buckling motion is thereby restricted was expected to alter the buckling of the beam, the magnitude of the effect of the spring being a function of the strength of the spring. Hayashi[14] showed that an elastic restraint at the center of an Euler column had just this effect. Small values of spring constant yielded critical loads close to, but higher than, the first mode critical load. As the spring value increased, the critical load increased until a point was reached where further increases in spring value failed to cause any increase in buckling load. The buckling load at large values of spring constant corresponded to the second mode critical load. A similar behavior was expected for the buckling of the deep beam and, indeed, was predicted in a theoretical study by Flint.[2]

Flint's equation reduces to

$$P_{cr} = \frac{17.2\sqrt{EIGJ(1+\lambda)}}{L^2} \qquad (4)$$

when a one term approximation to the deflected shape is used. All terms of this equation are the same as those given for equations (2) and (3), except that λ is defined as

$$\lambda = \frac{kL^3}{48EI}$$

and

k = spring constant of the elastic restraint.

Tables 3a through 3n and Figs. 9a through 9r show that the elastically restrained deep beam does, in fact, behave as expected. Fig. 9r shows a comparison between a one term approximation to the deformed shape in Flint's equation and the experimental results achieved.

An interesting piece of information evolved as the experimentation using elastic restraints progressed. Although the motion of the centroid became quite small as the spring constant reached values higher than about 20 pounds per inch, the Southwell presentations of this data continued to appear as indisputable straight lines even with springs with constants as high as 97.4 pounds per inch, as can be seen in Figs. 9b through 9p. But, as the spring constants exceeded 20 pounds per inch, the critical loads obtained from the Southwell plots resulting from the deflections of the centroid began to surpass the theoretical value predicted for second mode. It was visually observed that, beginning with spring values of about 10 pounds per inch, the beam began to deform, under loading, not in a pure first mode shape, but in a shape that suggested a combination of first and second modes. The transition from first mode, through this combination of first and second modes, to pure second mode is visible in Figs. 6a through 6c.

By constructing Southwell plots of the data measured at

the quarter points and comparing the critical loads determined from these plots with the data measured at the centroid, it became apparent that, as the value of the spring constant of the elastic restraint exceeded about 20 pounds per inch, the values of critical load determined from the quarter point data began to diverge considerably from those determined from the deflection data of the centroid. Whereas the buckling loads from the quarter point data leveled off at the theoretical critical value for second mode, the instability loads from the centroid deflection plots continued to increase to a high but erratic and indefinite value considerably in excess of the second mode critical load value.

Representative load-deflection curves for the centroid and quarter point measurements are shown in Figs. 9a, 9d, 9l and 9n, to show the effect of increasing spring value on deflection data. The corresponding Southwell plots appear in Figs. 9b, 9e, 9m, 9o and 9q.

The measurements at the quarter points were selected as the meaningful data for determining the critical loads of the elastically restrained beam because of several basic reasons. First, the critical loads determined from the quarter points level out at the theoretical second mode value as the spring constant approaches infinity. Second, the motion of the centroid is zero when the spring becomes infinitely large and therefore cannot be measured. The critical load cannot, then, be determined by measurements at the centroid when an infinite spring is present. Third, the fact that the Southwell presentation of data measured at the

centroid with relatively large spring values remains linear in form can be reasonably well explained by considering that the beam is locally deformed by the spring, and that the high critical load determinations from this data are probably higher mode tendencies of the beam in the vicinity of the local deformation. Fourth, if the development of mode shape is examined, it becomes apparent that with a predominant first mode deformation, the midpoint and quarter points of the beam exhibit a preponderance of first mode motion. But, when the beam is deformed primarily in second mode, the quarter points move considerably but the centroid alters position but little, if at all. Therefore, as the beam nears second mode, measurements at the centroid should not be expected to give adequate results since little or no second mode motion occurs there. Note, however, that if third mode motion is present to any degree, it will reveal itself to the greatest extent at the beam center. This is also true of all higher odd numbered modes. The effect of these modes is considered to be making itself evident in the data taken at the centroid when the springs of high strength are used.

Fig. 9r presents a graph of the ratio of buckling load divided by the critical load value of the unrestrained beam, $P_{cr}/P_{o_{cr}}$, versus the spring constant, k, of the elastic restraint imposed at the centroid. The results obtained by measuring the deflections at the centroid and at the quarter points are shown. The consistency of the data resulting from the latter measurements is evident. The experimental and theoretical stability boundaries

are shown in this figure and the comparison between theory and experiment for the case of the elastically restrained beam is clearly presented here.

Experimentation in the large deflection range produced the final link in the verification of the buckling equation (2). The large deflection hypothesis proposes that, if load is plotted against the square of deflection in the large deflection region (where the end of the beam assumes an angle of from five to thirty degrees from its undistorted position) a straight line will result in the post-buckling region, and that the intercept of this line with the line of zero deflection will yield the theoretical buckling load of the member tested. As has been mentioned before, the theory has been verified for an Euler column;[10] for some thermal buckling problems;[11] and for various flat plates.[12]

The first tests for large deflection data on the deep beam were performed on the beam used for small deflection data. It became apparent immediately that two major difficulties existed. First, the end supports, although adequate for small deflections, would not allow sufficient freedom for large deflection readings. Second, the beam material, a relatively low grade steel, entered the region of plastic deformation as soon as any appreciable deflection was attained.

The test apparatus shown in Figs. 7a through 7c provided an acceptable solution to the problem of the end supports. The beam first tested in this rig was made of fibreglass and had dimensions of 20.91 X 1.50 X 0.0345 inches. The advantage of the fibreglass material was that it possessed a high yield strength and

therefore remained elastic throughout considerable distortion. Tables 4a and 4b, and Figs. 10a through 10f indicate the results of the tests on this beam. The perplexing part of these results is that, for the glass beam, the small deflection buckling load obtained from the Southwell presentations is roughly 16 percent different from that resulting from the large deflection plots. The cause is believed to be the non-linear characteristics of the fibreglass material. Indeed, an appreciable amount of creep was observed when performing the tests, but it was also learned that the fibreglass material had a definite change in modulus as the stress passed a given value, this value lying between the stresses experienced by the material in the small and large deflection regions. One observation, however, proved of value, despite the obvious difficulties encountered in the tests of the glass beam. The same large deflection results were obtained whether the measurements were made at the centroid of the beam or at the top fibre. Since the deflection of the top fibre was much easier to measure, this knowledge was used on subsequent tests.

The next beam to be tested had dimensions of 20.91 X 1.50 X 0.0148 inches and was made of high grade spring steel. By using the moduli of the steel as $E = 3 \times 10^7$ psi and $G = 1.1 \times 10^7$ psi respectively, and calculating the theoretical critical load for first mode buckling by use of equation (2), a value of 0.573 pounds or 260 grams was obtained. Table 5 and Figs. 11a through 11c show the results of the tests on this beam. The buckling load by Southwell plot is seen to be 260.5 grams and by large deflection data to be 252 grams. The correlation is within about three percent.

VI. CONCLUSIONS

The work contained in this thesis experimentally verifies the theoretical determination of the lateral buckling load of a deep beam with a concentrated load at the centroid. The Southwell presentation of data is proven to be an excellent method of analysis of lateral instability in this case. In addition, as a means of further verification of both the purely theoretical and the Southwell arguments, the large deflection method is shown to produce an excellent three way correlation. All experimental data contained herein is within about three percent of theory, which is considered completely adequate.

To obtain suitable experimental accuracy, however, it was found that extreme care had to be exercised in imposing end conditions, in applying loads and in ascertaining that the beam materials possessed adequate elastic characteristics. Relatively small deviations from these requirements could result in considerable errors in experimental results.

The work, therefore, provides experimental verification of the theoretical equation for lateral instability load for a deep beam by using two methods which make a definitive prediction of buckling load.

REFERENCES

1. Timoshenko, S. P. and Gere, J. M.: Theory of Elastic Stability, 2nd ed., McGraw-Hill Book Company, Inc., New York, N. Y., 1961, pp. 251 - 272.

2. Flint, A. R.: The Influence of Restraints on the Stability of Beams, Structural Engineer, vol. 29, no. 9, Sept. 1951, pp. 235 - 246.

3. Bromley, S. and Robinson, W. H.: The Lateral Failure of Spars, NACA Technical Note No. 232, Mar. 1926.

4. Trayer, G. W. and March, H. W.: Elastic Instability of Members Having Sections Common in Aircraft Construction, NACA Technical Report No. 382, 1931.

5. Dumont, C. and Hill, H. N.: The Lateral Instability of Deep Rectangular Beams, NACA Technical Note No. 601, May, 1937.

6. Massey, C.: Southwell Plot Applied to Lateral Instability of Beams, Engineer, vol. 218, no. 5666, Aug. 1964, pp. 320.

7. Horton, W. H., Cundari, F. L. and Johnson, R. W.: A Review of the Applicability of the Southwell Plot to the Interpretation of Test Data Obtained from Studies of Elastic Column and Plate Structures, SUDAAR No. 296, Stanford University, Dec. 1966.

8. Southwell, R. V.: On the Analysis of Experimental Observations in Problems of Elastic Stability, Proceedings of the Royal Society, A, vol. 135, 1932, pp. 601 - 616.

9. Westergaard, H. M.: Buckling of Elastic Structures, Transactions of the American Society of Civil Engineers, vol. 85, 1922, pp. 576 - 654.

10. Horton, W. H., Tenerelli, D. J. and Willey, B. T.: The Use of Small and Large Displacement Data from Essentially Elastic Buckling Tests on Columns and Plates as a Means of Correlating Theory and Experiment, a paper presented at the SESA Spring Conference Ottawa, May 1967.

11. Queinec, A.: Thermal Buckling of Centrally Heated Circular Plates, SUDAAR No. 143, Stanford University, June 1961.

12. Willey, B. T.: The Instability of Glass Fibre Reinforced Plastic Panels Under Axial Compression, Engineers Thesis, Stanford University, 1967.

13. Horton, W. H., Bailey, S. C. and McQuilkin, B. H.: An Introduction to Instability (A Pictorial Survey of the Stability of Bars, Plates and Shell Bodies), a paper presented at the Sixty-Ninth Annual Meeting of the American Society for Testing and Materials, Atlantic City, N. J., June 1966.

14. Hayashi, T. and Kihira, M.: On a Method of Experimental Determination of the Buckling Load of an Elastically Supported Column, a paper presented at the Japan Congress on Testing Materials, Kyoto, Japan, Sept. 1966.

TABLE 1a

TEST DATA FOR BUCKLING OF EULER COLUMN
(INDIVIDUAL TESTS)

LOAD P (gm)	DEFLECTION δ (mm)		
	Test 1	Test 2	Test 3
0.0	0.0	0.0	0.0
77.5	0.0	0.0	0.0
159.0	0.0	0.0	0.0
259.0	0.2	0.2	0.3
309.0	0.6	0.6	0.6
329.0	0.8	0.9	0.9
349.0	1.0	1.1	1.2
369.0	2.0	2.1	2.1
389.0	4.9	5.4	5.4
394.0	7.3	7.9	8.1
399.0	11.8	12.0	12.2
400.0	12.8	13.1	13.2
402.0	15.0	15.1	15.3
403.0	15.9	16.1	16.2
403.5	16.3	16.7	16.8
404.0	17.0	17.2	17.2
405.0	18.0	18.1	18.2
406.0	18.9	19.1	19.1
408.0	20.6	20.9	21.0
410.0	22.4	22.4	22.6
412.0	24.1	24.1	23.9
414.0	25.4	25.5	25.4

TABLE 1b

TEST DATA FOR BUCKLING OF EULER COLUMN
(INDIVIDUAL TESTS)

LOAD P (gm)	DEFLECTION δ (mm)			
	Test 4	Test 5	Test 6	Test 7
0.0	0.0	0.0	0.0	0.0
77.5	0.0	0.0	0.0	0.0
159.0	0.0	0.0	0.0	0.0
259.0	0.2	0.3	0.3	0.3
309.0	0.5	0.7	0.7	0.7
329.0	0.9	0.9	0.9	1.0
349.0	1.2	1.3	1.4	1.5
369.0	2.1	2.3	2.5	2.6
389.0	5.6	5.8	6.0	6.1
391.0	6.3	6.9	6.8	7.0
393.0	7.6	7.9	8.0	8.1
395.0	8.9	9.1	9.4	9.5
395.5	9.3	9.6	9.6	9.8
396.0	9.8	10.0	10.1	10.1
397.0	10.5	10.8	11.0	11.0
399.0	12.3	12.7	12.7	12.9
401.0	14.5	14.7	14.6	14.8
406.0	19.2	19.4	19.3	19.5
407.0	20.1	20.2	20.3	20.3
409.0	21.8	21.8	21.8	21.9
411.0	23.3	23.3	23.3	23.5
413.0	24.7	24.8	24.8	24.9
414.0	25.4	25.6	25.5	25.6

TABLE 1c

AVERAGED DATA FOR BUCKLING OF
EULER COLUMN

P (gm)	δ (mm)	δ^2	δ/P
0.0	0.0	0.0	---
77.5	0.0	0.0	0.0
159.0	0.0	0.0	0.0
259.0	0.26	0.068	0.27×10^{-3}
309.0	0.63	0.395	1.28
329.0	0.90	0.81	2.46
349.0	1.24	1.54	4.4
369.0	2.24	5.0	6.1
389.0	5.60	31.3	14.4
391.0	6.75	45.5	17.3
393.0	7.90	62.2	20.1
394.0	7.78	60.5	19.7
395.0	9.22	84.9	23.3
396.0	10.0	100.0	25.2
397.0	10.8	117.0	27.2
399.0	12.7	162.0	31.8
400.0	13.2	174.0	33.0
401.0	14.7	216.0	36.7
402.0	15.1	228.0	37.6
403.0	16.1	260.0	40.0
404.0	17.1	293.0	42.3
405.0	18.1	327.0	44.7
406.0	19.2	369.0	47.3
407.0	20.2	408.0	49.7
408.0	20.8	432.0	51.0
409.0	21.8	475.0	53.4
410.0	22.5	503.0	54.9
411.0	23.4	549.0	56.9
412.0	24.0	576.0	58.3
413.0	24.8	615.0	60.0
414.0	25.5	650.0	61.6×10^{-3}

$$\frac{\Delta x}{\Delta y} = \frac{18.0}{44.0 \times 10^{-3}} = 409 \text{ gm} = P_{cr}$$

TABLE 2a

LATERAL BUCKLING OF DEEP BEAM WITHOUT ELASTIC RESTRAINT
(TEST No. 1)

LOAD P (lb)	DEFLECTION OF CENTROID δ (inches)	δ/P
0.0	0.0	---
7.70	0.001	1.299×10^{-4}
12.13	0.006	4.95
14.30	0.011	7.70
15.49	0.016	10.33
16.85	0.021	12.48
17.64	0.026	14.74
18.18	0.031	17.07
18.57	0.036	19.40
18.99	0.041	21.60
19.29	0.046	23.83
19.47	0.051	26.20
19.72	0.056	28.40
19.86	0.061	30.72
20.07	0.071	35.36
20.16	0.077	38.20
20.26	0.081	40.00
20.41	0.086	42.1
20.51	0.092	44.9
20.58	0.101	49.1
20.70	0.112	54.2
20.79	0.126	60.7
20.90	0.141	67.5
20.99	0.161	76.8
21.01	0.181	86.1
21.03	0.201	95.5
21.05	0.221	104.9×10^{-4}

$$\frac{\Delta x}{\Delta y} = \frac{0.28}{130.7 \times 10^{-4}} = 21.4 \text{ lb} = P_{o_{cr}}$$

TABLE 2b

LATERAL BUCKLING OF DEEP BEAM WITHOUT ELASTIC RESTRAINT
(TEST No. 2)

LOAD P (lb)	DEFLECTION OF CENTROID δ (inches)	δ/P
0.0	0.0	---
7.70	0.001	1.30×10^{-4}
12.17	0.006	4.93
14.59	0.011	7.55
15.85	0.016	9.47
17.10	0.021	12.29
17.85	0.026	14.58
18.28	0.031	16.97
18.70	0.036	19.25
19.11	0.041	21.45
19.32	0.046	23.80
19.62	0.051	26.00
19.79	0.056	28.30
19.90	0.061	30.65
20.05	0.066	32.92
20.11	0.071	34.80
20.25	0.076	37.50
20.32	0.081	39.9
20.42	0.086	42.1
20.50	0.091	44.4
20.55	0.096	46.8
20.58	0.101	49.1
20.60	0.106	51.5
20.67	0.116	56.2
20.71	0.126	60.9
20.79	0.137	66.0
20.81	0.151	72.5
20.89	0.171	81.9
20.92	0.191	91.4
20.93	0.211	100.9
20.99	0.231	110.0
21.01	0.241	114.7
21.02	0.261	124.0×10^{-4}

TABLE 3a

LATERAL BUCKLING OF DEEP BEAM WITH ELASTIC RESTRAINT AT CENTROID
(SPRING CONSTANT = 0.0 lb/in)

LOAD	LEFT QUARTER DEFLECTIONS		CENTROID DEFLECTIONS		RIGHT QUARTER DEFLECTIONS	
P (lb)	δ (inches)	δ/P	δ (inches)	δ/P	δ (inches)	δ/P
0.0	0.0		0.0		0.0	
1.20	0.0010		0.0		0.0003	
2.55	0.0014		0.003		0.0025	
4.85	0.0057		0.012		0.0074	
8.00	0.0102		0.019		0.0132	
11.3	0.0181		0.035	3.10×10^{-3}	0.0229	
13.2	0.0341	2.58×10^{-3}	0.060	4.55	0.0403	3.05×10^{-3}
14.1	0.0398	2.82	0.069	4.90	0.0467	3.30
14.85	0.0501	3.38	0.085	5.72	0.0582	3.93
15.2	0.0535	3.52	0.090	5.92	0.0617	4.05
15.8	0.0537	3.42	0.095	6.01	0.0643	4.075
16.16	0.0647	4.00	0.107	6.63	0.0734	4.54
16.3	0.0680	4.15	0.114	7.00	0.0777	4.75
16.6	0.0733	4.41	0.122	7.35	0.0831	5.01
16.8	0.0757	4.50	0.125	7.50	0.0861	5.125
17.0	0.0812	4.78	0.135	7.95	0.0923	5.43
17.1	0.0823	4.80	0.136	7.95	0.0941	5.50
17.3	0.0915	5.28	0.149	8.61	0.1028	5.93
17.6	0.0975	5.56	0.159	9.04	0.1092	6.24
17.8	0.1095	6.18	0.177	9.95	0.1215	6.84
17.9	0.1112	6.23	0.180	10.05	0.1239	6.94
18.0	0.1152	6.40×10^{-3}	0.186	10.33×10^{-3}	0.1279	7.10×10^{-3}
	$\frac{\Delta x}{\Delta y} = \frac{20\times10^{-2}}{9.49\times10^{-3}} = 21.1$ lb $= P_{o_{cr}}$		$\frac{\Delta x}{\Delta y} = \frac{20\times10^{-2}}{9.35\times10^{-3}} = 21.4$ lb $= P_{o_{cr}}$		$\frac{\Delta x}{\Delta y} = \frac{20\times10^{-2}}{9.33\times10^{-3}} = 21.4$ lb $= P_{o_{cr}}$	

TABLE 3b

LATERAL BUCKLING OF DEEP BEAM WITH ELASTIC RESTRAINT AT CENTROID
(SPRING CONSTANT = 1.17 lb/in)

LOAD	CENTROID DEFLECTIONS	
P (lb)	δ (inches)	δ/P
19.07	0.021	11.01×10^{-4}
24.45	0.061	24.96
25.40	0.091	35.81
26.16	0.126	48.22
26.67	0.161	60.43
27.00	0.203	75.20
27.18	0.251	92.40×10^{-4}

$$\frac{\Delta x}{\Delta y} = \frac{2.5 \times 10^{-1}}{89.1 \times 10^{-4}} = 28.06 \text{ lb} = P_{cr}$$

$$\frac{P_{cr}}{P_{o_{cr}}} = \frac{28.06}{21.4} = 1.31$$

TABLE 3c

LATERAL BUCKLING OF DEEP BEAM WITH ELASTIC RESTRAINT AT CENTROID
(SPRING CONSTANT = 3.18 lb/in)

LOAD P (lb)	CENTROID DEFLECTIONS	
	δ (inches)	δ/P
25.72	0.031	12.06×10^{-4}
29.33	0.051	17.39
31.95	0.091	28.48
32.52	0.111	34.13
33.31	0.151	45.32
33.73	0.191	56.70
33.90	0.211	62.25×10^{-4}

$$\frac{\Delta x}{\Delta y} = \frac{2.5 \times 10^{-1}}{70 \times 10^{-4}} = 35.7 \text{ lb} = P_{cr}$$

$$\frac{P_{cr}}{P_{o_{cr}}} = \frac{35.7}{21.4} = 1.67$$

TABLE 3d

LATERAL BUCKLING OF DEEP BEAM WITH ELASTIC RESTRAINT AT CENTROID
(SPRING CONSTANT = 4.64 lb/in)

LOAD	LEFT QUARTER DEFLECTIONS		CENTROID DEFLECTIONS		RIGHT QUARTER DEFLECTIONS	
P (lb)	δ (inches)	δ/P	δ (inches)	δ/P	δ (inches)	δ/P
0.0	0.0		0.0		0.0	
2.57	0.0		0.002		0.0010	
4.97	0.0005		0.005		0.0024	
8.00	0.0020		0.008		0.0037	
11.06	0.0030		0.012		0.0074	
13.10	0.0052		0.015		0.0089	
16.92	0.0068	0.402×10^{-3}	0.022	1.30×10^{-3}	0.0137	0.810×10^{-3}
20.41	0.0098	0.480	0.030	1.47	0.0187	0.916
23.48	0.0133	0.567	0.040	1.70	0.0256	1.138
26.71	0.0193	0.723	0.055	2.06	0.0351	1.314
29.88	0.0273	0.914	0.074	2.48	0.0468	1.566
31.53	0.0335	1.062	0.092	2.92	0.0588	1.865
33.50	0.0503	1.500	0.129	3.85	0.0828	2.470
34.24	0.0610	1.780	0.150	4.38	0.0955	2.788
34.67	0.0743	2.140	0.176	5.08	0.1116	3.218
35.15	0.0905	2.573×10^{-3}	0.203	5.78×10^{-3}	0.1271	3.620×10^{-3}
	$\frac{\Delta x}{\Delta y} = \frac{20\times10^{-2}}{5.125\times10^{-3}} = 39.05$ lb		$\frac{\Delta x}{\Delta y} = \frac{20\times10^{-2}}{5.05\times10^{-3}}$		$\frac{\Delta x}{\Delta y} = \frac{20\times10^{-2}}{4.965\times10^{-3}} = 40.28$ lb	
	$= P_{cr}$		$= 39.6$ lb $= P_{cr}$		$= P_{cr}$	
	$\frac{P_{cr}}{P_{o_{cr}}} = \frac{39.05}{21.4} = 1.83$		$\frac{P_{cr}}{P_{o_{cr}}} = \frac{39.6}{21.4} = 1.85$		$\frac{P_{cr}}{P_{o_{cr}}} = \frac{40.28}{21.4} = 1.88$	

TABLE 3e

LATERAL BUCKLING OF DEEP BEAM WITH ELASTIC RESTRAINT AT CENTROID
(SPRING CONSTANT = 9.75 lb/in)

LOAD	LEFT QUARTER DEFLECTIONS		CENTROID DEFLECTIONS		RIGHT QUARTER DEFLECTIONS	
P (lb)	δ (inches)	δ/P	δ (inches)	δ/P	δ (inches)	δ/P
0.0	0.0		0.0		0.0	
2.52	0.0		0.0		0.0	
4.85	0.0002		0.004		0.0015	
8.06	0.0010		0.006		0.0029	
10.92	0.0005		0.007		0.0040	
13.95	0.0006		0.009	0.645×10^{-3}	0.0054	0.387×10^{-3}
17.05	0.0015	0.088×10^{-3}	0.014	0.821	0.0078	0.507
20.24	0.0019	0.094	0.017	0.840	0.0105	0.519
23.37	0.0025	0.107	0.022	0.942	0.0136	0.582
26.6	0.0041	0.154	0.028	1.052	0.0187	0.703
29.8	0.0051	0.171	0.036	1.208	0.0233	0.782
32.87	0.0067	0.204	0.047	1.430	0.0311	0.945
36.05	0.0099	0.274	0.062	1.730	0.0403	1.119
39.18	0.0145	0.370	0.087	2.220	0.0563	1.438
41.13	0.0181	0.440	0.108	2.628	0.0683	1.660
42.9	0.0250	0.583	0.140	3.262	0.0872	2.035
43.8	0.0300	0.685	0.161	3.678	0.0978	2.232
44.5	0.0365	0.820	0.188	4.222	0.1133	2.548
44.9	0.0398	0.888×10^{-3}	0.206	4.595×10^{-3}	0.1232	2.746×10^{-3}
	$\frac{\Delta x}{\Delta y} = \frac{4\times10^{-2}}{0.824\times10^{-3}} = 48.6$ lb $= P_{cr}$		$\frac{\Delta x}{\Delta y} = \frac{20\times10^{-2}}{3.97\times10^{-3}} = 50.4$ lb $= P_{cr}$		$\frac{\Delta x}{\Delta y} = \frac{20\times10^{-2}}{3.925\times10^{-3}} = 51.0$ lb $= P_{cr}$	
	$\frac{P_{cr}}{P_{o_{cr}}} = \frac{48.6}{21.4} = 2.27$		$\frac{P_{cr}}{P_{o_{cr}}} = \frac{50.4}{21.4} = 2.36$		$\frac{P_{cr}}{P_{o_{cr}}} = \frac{51.0}{21.4} = 2.38$	

TABLE 3f

LATERAL BUCKLING OF DEEP BEAM WITH ELASTIC RESTRAINT AT CENTROID
(SPRING CONSTANT = 12.5 lb/in)

LOAD P (lb)	CENTROID DEFLECTIONS	
	δ (inches)	δ/P
0.0	0.0	
16.60	0.012	
22.09	0.022	
29.18	0.037	
35.53	0.063	1.77×10^{-3}
38.62	0.081	2.10
41.40	0.107	2.59
42.90	0.118	2.75
43.63	0.127	2.91
44.00	0.137	3.12
44.50	0.147	3.30
45.20	0.157	3.48×10^{-3}

$$\frac{\Delta x}{\Delta y} = \frac{19 \times 10^{-2}}{3.43 \times 10^{-3}} = 55.5 \text{ lb} = P_{cr}$$

$$\frac{P_{cr}}{P_{o_{cr}}} = \frac{55.5}{21.4} = 2.59$$

TABLE 3g

LATERAL BUCKLING OF DEEP BEAM WITH ELASTIC RESTRAINT AT CENTROID
(SPRING CONSTANT = 15.4 lb/in)

LOAD	LEFT QUARTER DEFLECTIONS		CENTROID DEFLECTIONS		RIGHT QUARTER DEFLECTIONS	
P (lb)	δ (inches)	δ/P	δ (inches)	δ/P	δ (inches)	δ/P
0.0	0.0		0.0		0.0	
2.57	0.0		0.0		0.0007	
4.90	0.0		0.001		0.0016	
7.95	0.0		0.003		0.0024	
11.05	0.0		0.004		0.0032	
14.11	0.0001		0.004		0.0036	
17.23	0.0004		0.007		0.0055	
20.50	0.0003		0.010		0.0075	
23.54	0.0007		0.013		0.0087	0.370×10^{-3}
26.77	0.0011		0.016	0.599×10^{-3}	0.0119	0.445
29.98	0.0016	0.053×10^{-3}	0.020	0.668	0.0150	0.503
33.32	0.0026	0.078	0.025	0.751	0.0192	0.578
36.22	0.0037	0.102	0.033	0.920	0.0238	0.657
39.38	0.0054	0.1376	0.042	1.066	0.0310	0.780
42.65	0.0091	0.213	0.054	1.265	0.0394	0.924
45.6	0.0161	0.353	0.073	1.600	0.0541	1.186
48.1	0.0240	0.498	0.098	2.035	0.0723	1.500
49.9	0.0327	0.656	0.125	2.507	0.0936	1.880
50.8	0.0402	0.791	0.152	2.993	0.1126	2.215
51.5	0.0473	0.919	0.180	3.500	0.1343	2.610
51.8	0.0494	0.953×10^{-3}	0.195	3.765×10^{-3}	0.1446	2.790×10^{-3}
	$\frac{\Delta x}{\Delta y} = \frac{4.5\times10^{-2}}{8.16\times10^{-4}} = 55.1$ lb $= P_{cr}$		$\frac{\Delta x}{\Delta y} = \frac{20\times10^{-2}}{3.55\times10^{-3}} = 56.4$ lb $= P_{cr}$		$\frac{\Delta x}{\Delta y} = \frac{20\times10^{-2}}{3.54\times10^{-3}} = 56.5$ lb $= P_{cr}$	
	$\frac{P_{cr}}{P_{o_{cr}}} = \frac{55.1}{21.4} = 2.58$		$\frac{P_{cr}}{P_{o_{cr}}} = \frac{56.4}{21.4} = 2.63$		$\frac{P_{cr}}{P_{o_{cr}}} = \frac{56.5}{21.4} = 2.64$	

TABLE 3h

LATERAL BUCKLING OF DEEP BEAM WITH ELASTIC RESTRAINT AT CENTROID
(SPRING CONSTANT = 20.0 lb/in)

LOAD	LEFT QUARTER DEFLECTIONS		CENTROID DEFLECTIONS		RIGHT QUARTER DEFLECTIONS	
P (lb)	δ (inches)	δ/P	δ (inches)	δ/P	δ (inches)	δ/P
0.0	0.0		0.0		0.0	
2.57	0.0002		0.0		0.0	
4.87	0.0004		0.002		0.0011	
7.95	0.0003		0.003		0.0019	
11.00	0.0005		0.004		0.0022	
14.09	0.0009		0.006		0.0030	
20.44	0.0019		0.010		0.0054	
26.65	0.0026		0.016		0.0101	0.417×10^{-3}
33.0	0.0055	0.167×10^{-3}	0.023	0.697×10^{-3}	0.0154	0.467
39.3	0.0118	0.301	0.035	0.891	0.0254	0.621
42.6	0.0175	0.410	0.043	1.009	0.0339	0.795
45.6	0.0270	0.592	0.055	1.205	0.0462	1.013
48.8	0.0437	0.896	0.073	1.497	0.0658	1.350
50.5	0.0575	1.138	0.084	1.664	0.0817	1.619
52.2	0.0942	1.794	0.112	2.147	0.1265	2.422
52.7	0.1026	1.947	0.117	2.22	0.1353	2.570
53.2	0.1365	2.568	0.133	2.50	0.1778	3.340
53.3	0.1459	2.739	0.139	2.61	0.1873	3.515
53.6	0.1529	2.85	0.143	2.67	0.1940	3.617
53.9	0.1557	2.89	0.147	2.73	0.1969	3.655
54.3	0.1595	2.94×10^{-3}	0.157	2.89×10^{-3}	0.2141	3.947×10^{-3}
	$\frac{\Delta x}{\Delta y} = \frac{20\times10^{-2}}{3.63\times10^{-3}} = 55.1$ lb		$\frac{\Delta x}{\Delta y} = \frac{20\times10^{-2}}{3.296\times10^{-3}}$		$\frac{\Delta x}{\Delta y} = \frac{20\times10^{-2}}{3.422\times10^{-3}} = 58.45$ lb	
	$= P_{cr}$		$= 60.75$ lb $= P_{cr}$		$= P_{cr}$	
	$\frac{P_{cr}}{P_{o_{cr}}} = \frac{55.1}{21.4} = 2.58$		$\frac{P_{cr}}{P_{o_{cr}}} = \frac{60.75}{21.4} = 2.84$		$\frac{P_{cr}}{P_{o_{cr}}} = \frac{58.45}{21.4} = 2.73$	

TABLE 3i

LATERAL BUCKLING OF DEEP BEAM WITH ELASTIC RESTRAINT AT CENTROID
(SPRING CONSTANT = 23.9 lb/in)

LOAD	LEFT QUARTER DEFLECTIONS		CENTROID DEFLECTIONS		RIGHT QUARTER DEFLECTIONS	
P (lb)	δ (inches)	δ/P	δ (inches)	δ/P	δ (inches)	δ/P
0.0	0.0		0.0		0.0	
2.59	0.0		0.0		0.0	
4.97	0.0		0.001		0.0003	
7.99	0.0002		0.002		0.0008	
11.04	0.0004		0.003		0.0018	
14.16	0.0007		0.004		0.0028	
20.48	0.0016		0.007		0.0054	
26.78	0.0045	0.168×10^{-3}	0.012	0.449×10^{-3}	0.0086	0.322×10^{-3}
33.00	0.0077	0.233	0.017	0.515	0.0135	0.410
38.35	0.0154	0.402	0.025	0.652	0.0217	0.566
45.65	0.0330	0.723	0.039	0.854	0.0386	0.845
48.80	0.0515	1.055	0.050	1.025	0.0564	1.154
51.80	0.0949	1.830	0.066	1.275	0.0990	1.91
53.65	0.1504	2.800	0.080	1.490	0.1537	2.86
53.9	0.1556	2.890	0.081	1.504	0.1596	2.96
54.0	0.1644	3.045	0.083	1.538	0.1688	3.12
54.4	0.1854	3.412	0.087	1.600	0.1913	3.52
54.7	0.2093	3.825	0.092	1.682	0.2170	3.97
55.0	0.2214	4.023	0.095	1.727	0.2298	4.18
55.2	0.2354	4.260×10^{-3}	0.098	1.775×10^{-3}	0.2447	4.44×10^{-3}
	$\frac{\Delta x}{\Delta y} = \frac{20\times10^{-2}}{3.432\times10^{-3}} = 58.3$ lb $= P_{cr}$		$\frac{\Delta x}{\Delta y} = \frac{20\times10^{-2}}{3.105\times10^{-3}} = 64.5 = P_{cr}$		$\frac{\Delta x}{\Delta y} = \frac{20\times10^{-2}}{3.486\times10^{-3}} = 57.4$ lb $= P_{cr}$	
	$\frac{P_{cr}}{P_{ocr}} = \frac{58.3}{21.4} = 2.72$		$\frac{P_{cr}}{P_{ocr}} = \frac{64.5}{21.4} = 3.01$		$\frac{P_{cr}}{P_{ocr}} = \frac{57.4}{21.4} = 2.68$	

TABLE 3j

LATERAL BUCKLING OF DEEP BEAM WITH ELASTIC RESTRAINT AT CENTROID
(SPRING CONSTANT = 34.0 lb/in)

LOAD	LEFT QUARTER DEFLECTIONS	
P (lb)	δ (inches)	δ/P
0.0	0.0	
2.57	0.0	
4.87	0.0008	
7.92	0.0010	
10.99	0.0018	
14.00	0.0029	
17.19	0.0044	0.256×10^{-3}
26.7	0.0086	0.322
33.0	0.0134	0.406
42.5	0.0321	0.755
45.6	0.0445	0.976
50.4	0.0854	1.695
52.2	0.1107	2.12
53.4	0.1425	2.67
54.4	0.1860	3.42
55.4	0.2283	4.13
55.7	0.2598	4.66
56.1	0.2740	4.88
56.3	0.2920	5.19
56.5	0.3045	5.39
56.6	0.3096	5.47×10^{-3}

$$\frac{\Delta x}{\Delta y} = \frac{30 \times 10^{-2}}{5.13 \times 10^{-3}} = 58.5 \text{ lb} = P_{cr}$$

$$\frac{P_{cr}}{P_{o_{cr}}} = \frac{58.5}{21.4} = 2.73$$

LOAD	CENTROID DEFLECTIONS	
P (lb)	δ (inches)	δ/P
0.0	0.0	
2.57	0.0	
4.87	0.0	
7.92	0.001	
10.99	0.001	
14.00	0.002	
17.19	0.005	
20.40	0.007	
23.45	0.007	
26.7	0.009	0.337×10^{-3}
29.9	0.010	0.334
33.0	0.013	0.394
39.4	0.018	0.457
45.5	0.027	0.594
50.4	0.037	0.735
53.4	0.043	0.806
54.7	0.048	0.878
56.1	0.053	0.945
56.5	0.056	0.991
56.6	0.056	0.990×10^{-3}

$$\frac{\Delta x}{\Delta y} = \frac{4 \times 10^{-2}}{0.558 \times 10^{-3}} = 71.7 \text{ lb} = P_{cr}$$

$$\frac{P_{cr}}{P_{o_{cr}}} = \frac{71.7}{21.4} = 3.35$$

TABLE 3k

LATERAL BUCKLING OF DEEP BEAM WITH ELASTIC RESTRAINT AT CENTROID
(SPRING CONSTANT = 50.5 lb/in)

LOAD	LEFT QUARTER DEFLECTIONS	
P (lb)	δ (inches)	δ/P
0.0	0.0	
2.57	0.0006	
4.92	0.0006	
7.96	0.0015	
11.0	0.0020	
14.0	0.0036	
17.2	0.0047	
20.4	0.0061	0.299×10^{-3}
33.0	0.0162	0.490
42.5	0.0371	0.873
45.5	0.0514	1.130
48.7	0.0767	1.576
51.2	0.1136	2.220
52.9	0.1530	2.895
54.4	0.2029	3.73
55.1	0.2626	4.77
55.7	0.2922	5.25
56.1	0.3196	5.70×10^{-3}

$$\frac{\Delta x}{\Delta y} = \frac{30\times10^{-2}}{5.13\times10^{-3}} = 58.5 \text{ lb} = P_{cr}$$

$$\frac{P_{cr}}{P_{o_{cr}}} = \frac{58.5}{21.4} = 2.73$$

LOAD	CENTROID DEFLECTIONS	
P (lb)	δ (inches)	δ/P
0.0	0.0	
2.57	0.001	
4.92	0.002	
7.96	0.002	
11.04	0.003	
14.0	0.002	
16.7	0.003	
20.4	0.007	
23.5	0.005	
26.7	0.008	0.300×10^{-3}
29.9	0.009	0.301
33.0	0.010	0.303
36.6	0.012	0.328
39.2	0.014	0.357
42.5	0.017	0.400
45.5	0.019	0.418
50.4	0.025	0.497
52.1	0.027	0.518
53.7	0.029	0.540
55.2	0.032	0.580
55.7	0.033	0.593
56.1	0.034	0.606×10^{-3}

$$\frac{\Delta x}{\Delta y} = \frac{4\times10^{-2}}{0.499\times10^{-3}} = 80.2 \text{ lb} = P_{cr}$$

$$\frac{P_{cr}}{P_{o_{cr}}} = \frac{80.2}{21.4} = 3.75$$

TABLE 31

LATERAL BUCKLING OF DEEP BEAM WITH ELASTIC RESTRAINT AT CENTROID
(SPRING CONSTANT = 97.4 lb/in)

LOAD	LEFT QUARTER DEFLECTIONS	
P (lb)	δ (inches)	δ/P
0.0	0.0	
2.59	0.0	
4.94	0.0001	
7.96	0.0006	
11.06	0.0021	
14.4	0.0038	
17.3	0.0046	
20.6	0.0061	
23.7	0.0070	
26.8	0.0100	0.374×10^{-3}
36.8	0.0203	0.552
42.7	0.0364	0.854
45.7	0.0511	1.12
49.0	0.0730	1.49
51.5	0.1085	2.11
52.8	0.1374	2.60
53.7	0.1681	3.13
54.5	0.2097	3.84
54.7	0.2420	4.43
55.2	0.2674	4.85
55.7	0.2981	5.35
56.1	0.3162	5.65×10^{-3}

$$\frac{\Delta x}{\Delta y} = \frac{30 \times 10^{-2}}{5.13 \times 10^{-3}} = 58.5 \text{ lb} = P_{cr}$$

$$\frac{P_{cr}}{P_{o_{cr}}} = \frac{58.5}{21.4} = 2.73$$

LOAD	CENTROID DEFLECTIONS	
P (lb)	δ (inches)	δ/P
0.0	0.0	
2.59	0.0	
4.97	0.0	
7.96	0.0	
11.06	0.0	
14.12	0.0002	
17.32	0.0002	
20.58	0.0002	
23.8	0.0011	0.0462×10^{-3}
26.8	0.0013	0.0485
30.0	0.0019	0.0634
33.2	0.0025	0.0753
36.4	0.0030	0.0825
39.4	0.0037	0.0940
42.7	0.0042	0.0984
46.7	0.0053	0.1136
49.0	0.0063	0.1285
50.7	0.0076	0.1500
51.5	0.0071	0.1380
52.3	0.0075	0.1434
52.8	0.0082	0.1550
53.2	0.0082	0.1540
53.7	0.0084	0.1565
53.8	0.0082	0.1525
54.1	0.0086	0.1590×10^{-3}

$$\frac{\Delta x}{\Delta y} = \frac{1 \times 10^{-2}}{0.138 \times 10^{-3}} = 72.5 \text{ lb} = P_{cr}$$

$$\frac{P_{cr}}{P_{o_{cr}}} = \frac{72.5}{21.4} = 3.38$$

TABLE 3m

LATERAL BUCKLING OF DEEP BEAM WITH ELASTIC RESTRAINT AT CENTROID
(SPRING CONSTANT = 155 lb/in)

LOAD	LEFT QUARTER DEFLECTIONS		LOAD	CENTROID DEFLECTIONS	
P (lb)	δ (inches)	δ/P	P (lb)	δ (inches)	δ/P
0.0	0.0		0.0	0.0	
2.57	0.0005		2.57	0.0	
4.90	0.0010		4.90	0.0	
7.92	0.0019		7.92	0.0	
10.95	0.0034		10.92	0.0	
14.0	0.0050		12.94	0.0	
17.1	0.0059		17.06	0.0	
20.2	0.0071		20.33	0.001	0.049×10^{-3}
23.4	0.0085	0.363×10^{-3}	23.42	0.001	0.043
36.2	0.0240	0.682	26.7	0.002	0.075
42.4	0.0406	0.958	29.9	0.002	0.067
45.5	0.0570	1.25	33.0	0.003	0.091
48.7	0.0796	1.64	36.2	0.004	0.111
50.4	0.1005	1.99	39.2	0.004	0.102
51.2	0.1153	2.26	42.5	0.005	0.118
52.0	0.1295	2.49	45.5	0.006	0.132
52.8	0.1590	3.01	48.7	0.007	0.144
53.7	0.1872	3.49	50.4	0.008	0.159
54.6	0.2291	4.20	51.1	0.008	0.157
55.0	0.2770	5.04	52.0	0.009	0.173
55.6	0.3115	5.60	52.9	0.009	0.170
55.9	0.3390	6.07×10^{-3}	53.3	0.010	0.188×10^{-3}
$\frac{\Delta x}{\Delta y} = \frac{30\times10^{-2}}{5.13\times10^{-3}} = 58.5$ lb $= P_{cr}$			$\frac{\Delta x}{\Delta y} = \frac{9\times10^{-3}}{0.122\times10^{-3}} = 73.8$ lb $= P_{cr}$		
$\frac{P_{cr}}{P_{o_{cr}}} = \frac{58.5}{21.4} = 2.73$			$\frac{P_{cr}}{P_{o_{cr}}} = \frac{73.8}{21.4} = 3.45$		

TABLE 3n

LATERAL BUCKLING OF DEEP BEAM WITH ELASTIC RESTRAINT AT CENTROID
(SPRING CONSTANT = ∞ lb/in)

LOAD P (lb)	LEFT QUARTER DEFLECTIONS	
	δ (inches)	δ/P
0.0	0.0	
2.57	0.0001	
4.92	0.0005	
7.97	0.0015	
11.01	0.0025	
14.11	0.0035	
17.14	0.0048	
20.4	0.0064	
23.5	0.0094	0.400×10^{-3}
26.7	0.0120	0.450
29.9	0.0145	0.485
33.0	0.0190	0.575
36.2	0.0238	0.658
39.2	0.0325	0.829
42.5	0.0415	0.977
45.5	0.0555	1.220
48.7	0.0810	1.665
50.4	0.1000	1.986
51.1	0.1104	2.16
52.0	0.1342	2.58
52.9	0.1608	3.04
53.3	0.1683	3.16
53.7	0.1841	3.48
54.2	0.2022	3.74
55.0	0.2402	4.37
55.2	0.2530	4.59
55.5	0.2640	4.76
55.7	0.2765	4.97
56.0	0.2988	5.33
56.2	0.3106	5.53×10^{-3}

$$\frac{\Delta x}{\Delta y} = \frac{30 \times 10^{-2}}{5.13 \times 10^{-3}} = 58.5 \text{ lb} = P_{cr}$$

$$\frac{P_{cr}}{P_{o_{cr}}} = \frac{58.5}{21.4} = 2.73$$

TABLE 4a

DEFLECTION DATA OF FIBREGLASS BEAM MEASURED AT CENTROID

LOAD P (gm)	DEFLECTION δ (inches)	δ/P	δ^2	LOAD P (gm)	DEFLECTION δ (inches)	δ^2
8	0.0	---		368	2.315	5.35
58	0.030	0.517×10^{-3}		378	2.410	5.80
78	0.048	0.615		388	2.493	6.20
108	0.085	0.787	0.0072	398	2.558	6.54
158	0.170	1.075		408	2.660	7.08
188	0.240	1.276		418	2.748	7.55
208	0.352	1.69	0.124	428	2.800	7.84
228	0.480	2.10		438	2.887	8.33
248	0.720	2.90		448	2.928	8.57
258	0.833	3.22×10^{-3}	0.690	458	2.968	8.80
278	1.133		1.282	468	3.055	9.30
298	1.425		2.03	478	3.110	9.67
308	1.598		2.55	488	3.175	10.08
318	1.748		3.06	498	3.198	10.20
328	1.860		3.46	508	3.238	10.48
338	2.005		4.02	518	3.262	10.63
348	2.100		4.41	528	3.280	10.77
358	2.200		4.84	538	3.295	10.84

$$\frac{\Delta x}{\Delta y} = \frac{0.8}{2.64 \times 10^{-3}} = 303 \text{ gm} = P_{ocr}$$

TABLE 4b

DEFLECTION DATA OF FIBREGLASS BEAM MEASURED AT TOP FIBRE

LOAD P (gm)	DEFLECTION (inches)	δ/P	δ^2	LOAD P (gm)	DEFLECTION δ (inches)	δ^2
7	0.0	---		327	2.220	4.93
57	0.039	0.684×10^{-3}		337	2.370	5.60
77	0.058	0.752		347	2.490	6.40
97	0.082	0.845	0.0067	357	2.600	6.76
117	0.112	0.958		367	2.700	7.30
127	0.129	1.016		377	2.830	8.00
137	0.149	1.088		387	2.990	8.92
147	0.169	1.150		397	3.070	9.41
157	0.193	1.230		407	3.190	10.20
167	0.222	1.330		417	3.300	10.90
177	0.252	1.423		427	3.400	11.57
187	0.296	1.583		437	3.490	12.19
197	0.346	1.757	0.1197	447	3.575	12.78
207	0.399	1.927		457	3.650	13.33
217	0.470	2.165		467	3.700	13.70
227	0.565	2.488		477	3.740	14.00
237	0.674	2.84		487	3.780	14.30
242	0.739	3.05		497	3.820	14.60
247	0.799	3.23×10^{-3}		507	3.850	14.80
257	0.990		0.978	517	3.920	15.37
277	1.330		1.77	527	3.970	15.77
297	1.725		2.98	537	3.990	15.92
307	1.940		3.76	547	4.005	16.03
317	2.090		4.36			

$$\frac{\Delta x}{\Delta y} = \frac{0.8}{2.69 \times 10^{-3}} = 297 \text{ gm} = P_{ocr}$$

TABLE 5

DEFLECTION DATA OF SPRING STEEL BEAM

LOAD P (gm)	DEFLECTION δ (inches)	δ/P	δ^2	LOAD P (gm)	DEFLECTION δ (inches)	δ^2
8	0.0	---		308	1.605	2.57
58	0.012	0.207×10^{-3}	0.00014	318	1.760	3.10
78	0.015	0.192		328	1.873	3.50
98	0.023	0.235		338	2.040	4.15
118	0.032	0.271		348	2.147	4.60
128	0.049	0.382		358	2.250	5.06
138	0.063	0.456		368	2.363	5.59
148	0.074	0.500		378	2.430	5.90
158	0.086	0.544	0.0074	388	2.540	6.42
168	0.100	0.595		398	2.640	6.98
178	0.117	0.658		408	2.728	7.43
188	0.141	0.750		418	2.820	7.92
198	0.172	0.870		428	2.880	8.28
208	0.219	1.051	0.0478	438	2.960	8.76
218	0.284	1.301		448	3.040	9.22
228	0.385	1.688×10^{-3}		458	3.133	9.80
238	0.513		0.263	468	3.201	10.25
248	0.685		0.469	478	3.227	10.40
258	0.840		0.704	488	3.268	10.66
268	1.030		1.060	498	3.290	10.80
278	1.190		1.42	508	3.318	10.99
288	1.350		1.82	518	3.340	11.14
298	1.465		2.15	528	3.362	11.30

$$\frac{\Delta x}{\Delta y} = \frac{0.4}{1.536 \times 10^{-3}} = 260.5 \text{ gm} = P_{ocr}$$

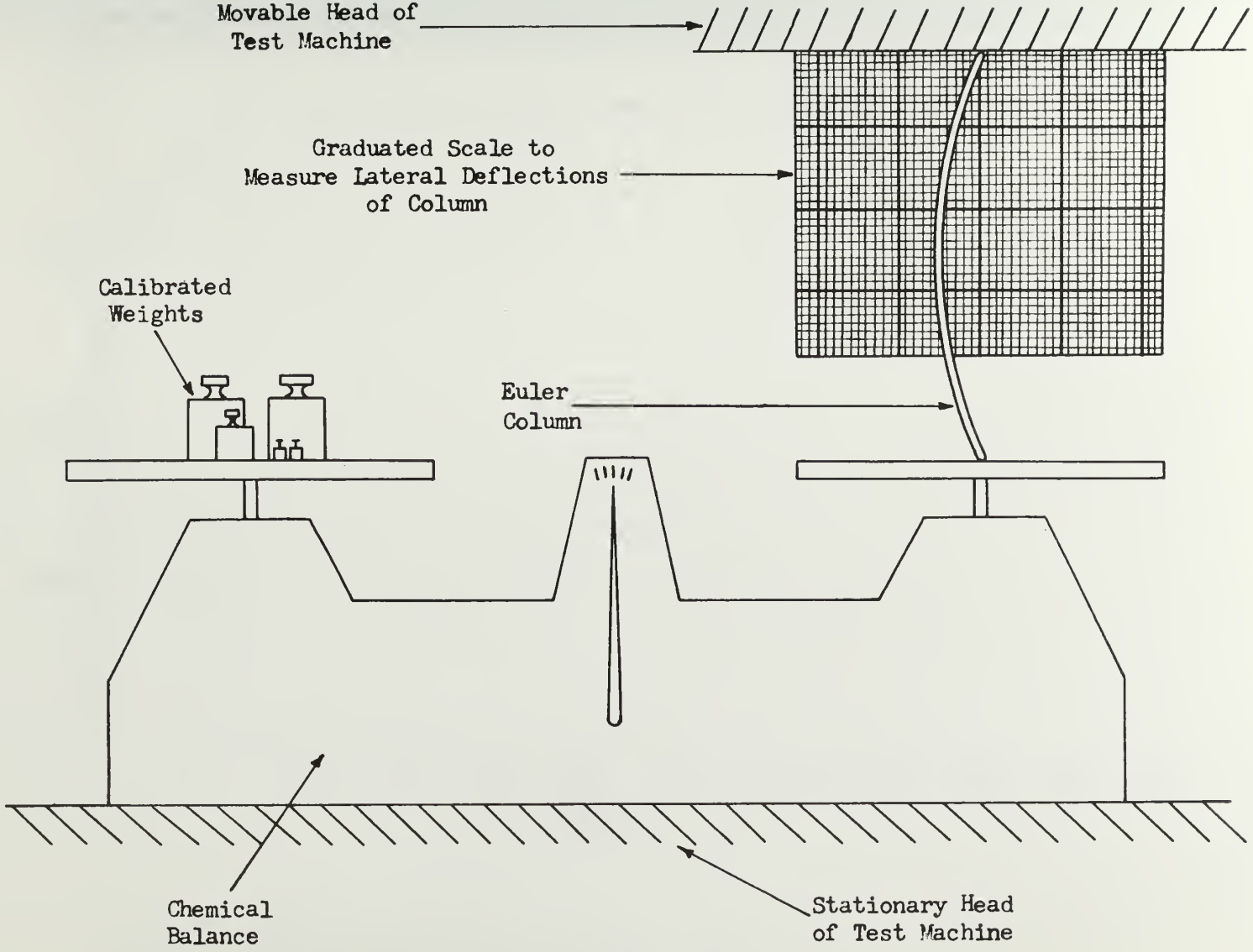

Fig. 1. Sketch of Test Rig Used to Experimentally Determine Buckling Load of Simply Supported Euler Column

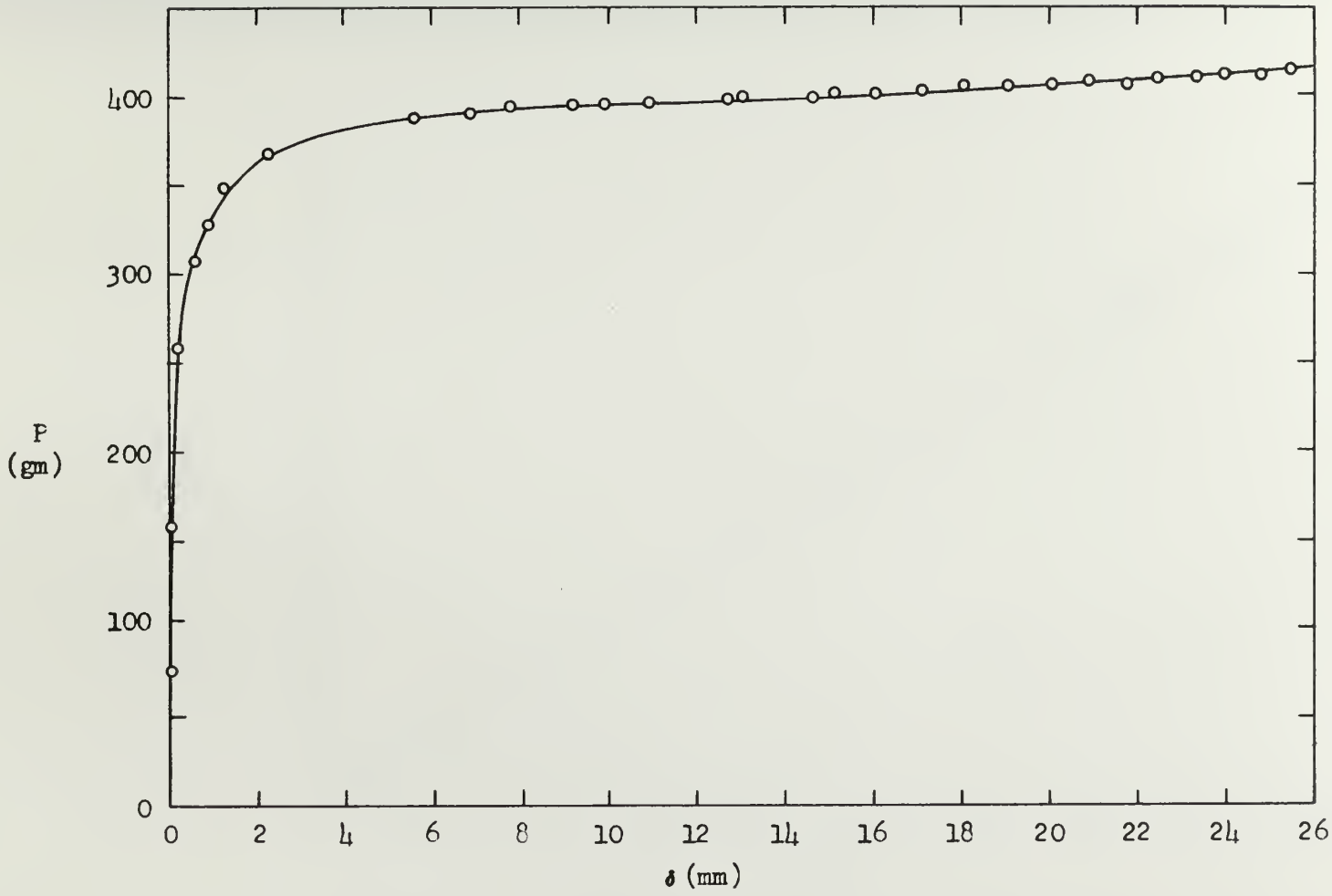

Fig. 2a. Load-Deflection Curve for Euler Column

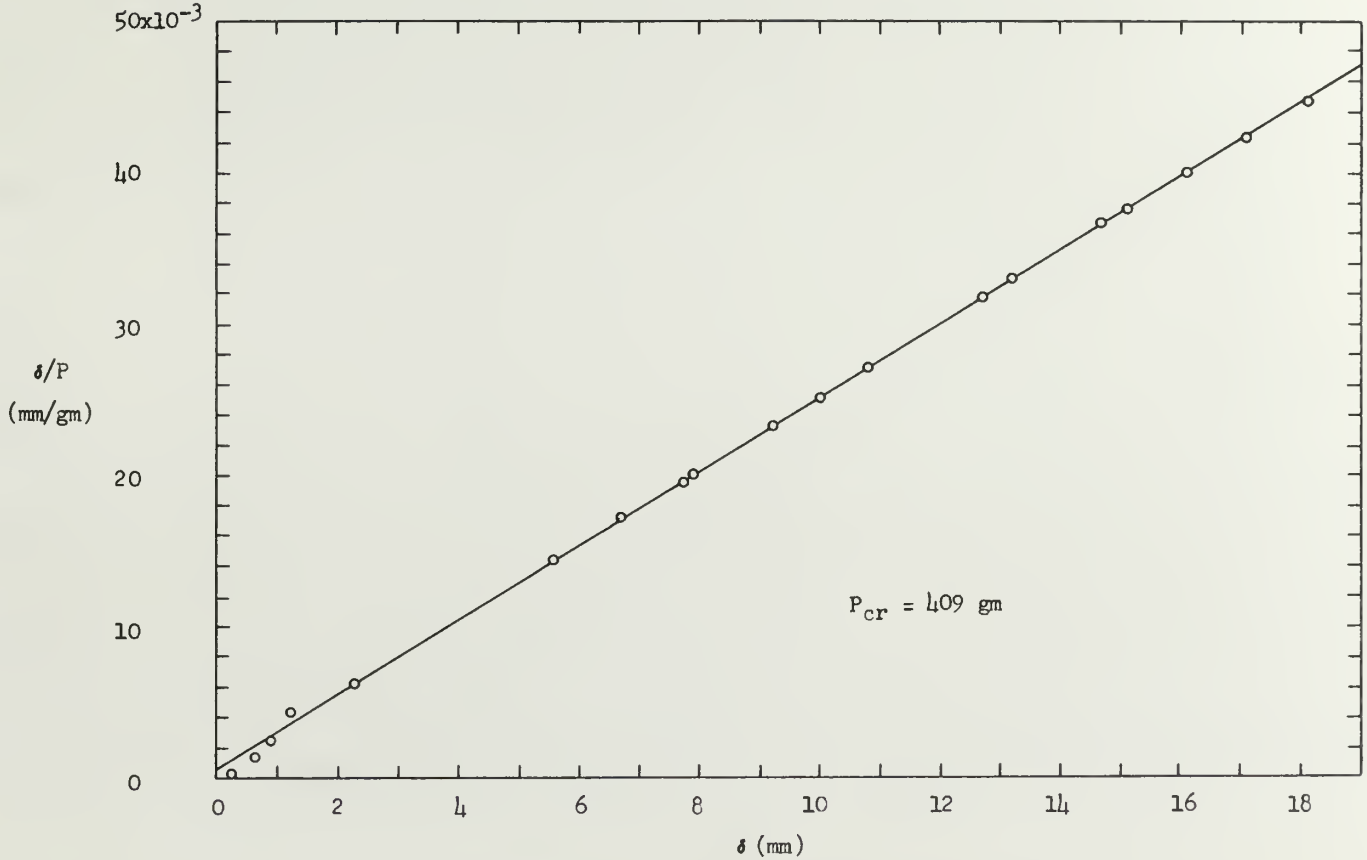

Fig. 2b. Southwell Plot for Buckling of Euler Column

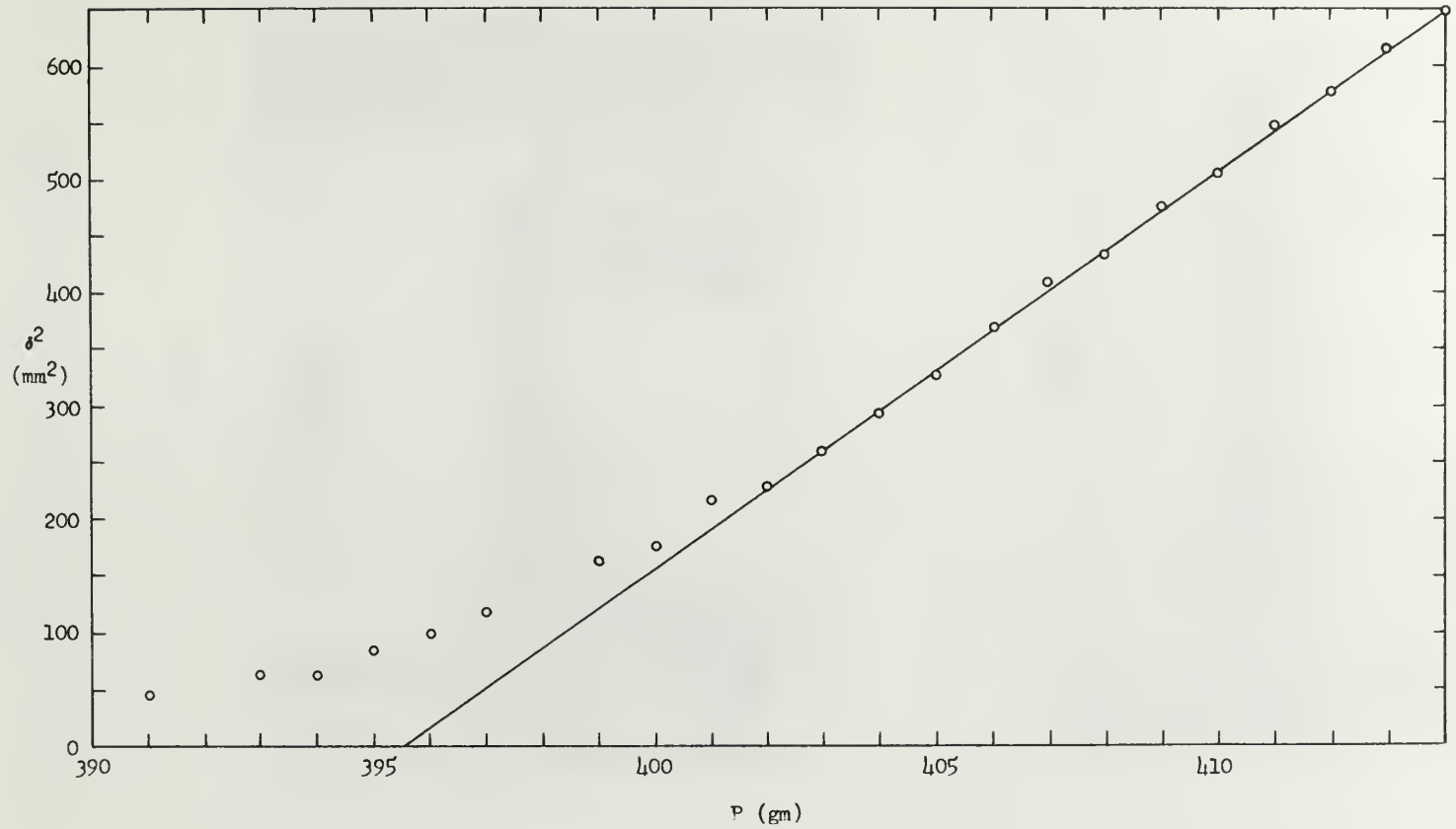

Fig. 2c. Large Deflection Plot for Euler Column

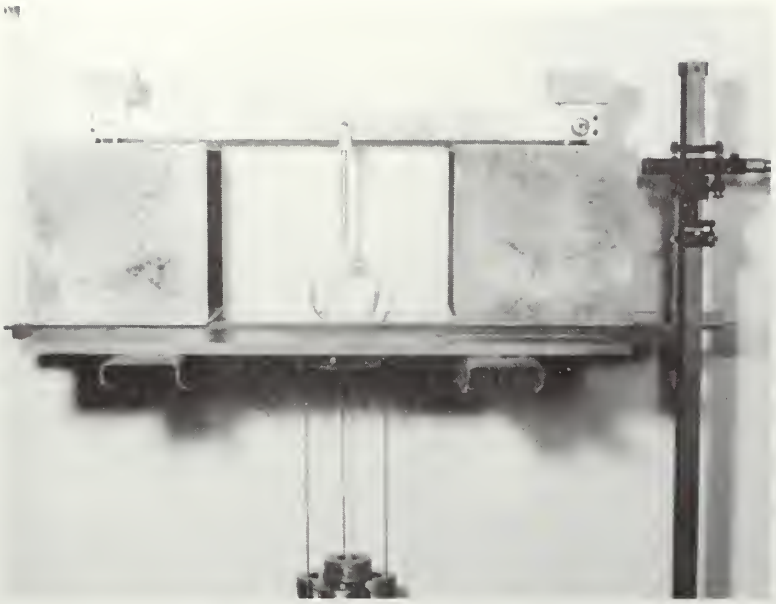

Fig. 3a.

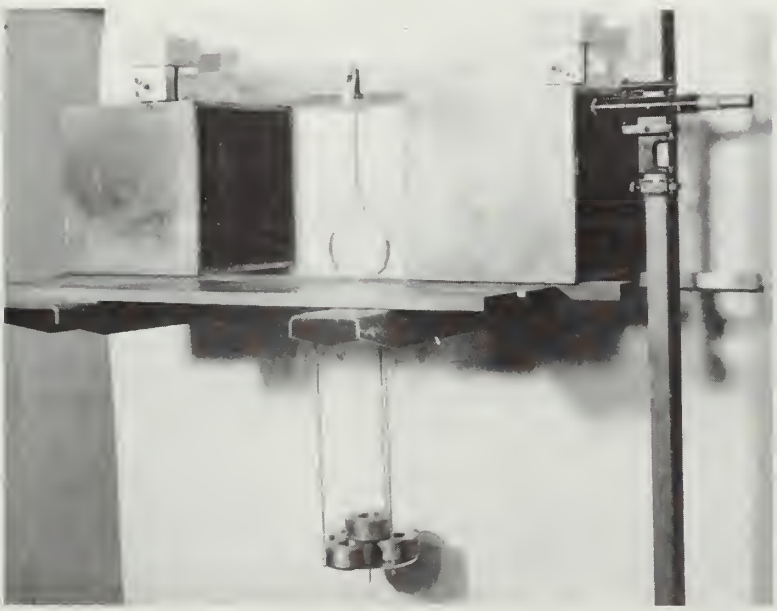

Fig. 3b.

Fig. 3. Apparatus Used for Small Deflection Tests of Lateral Instability of Deep Beam

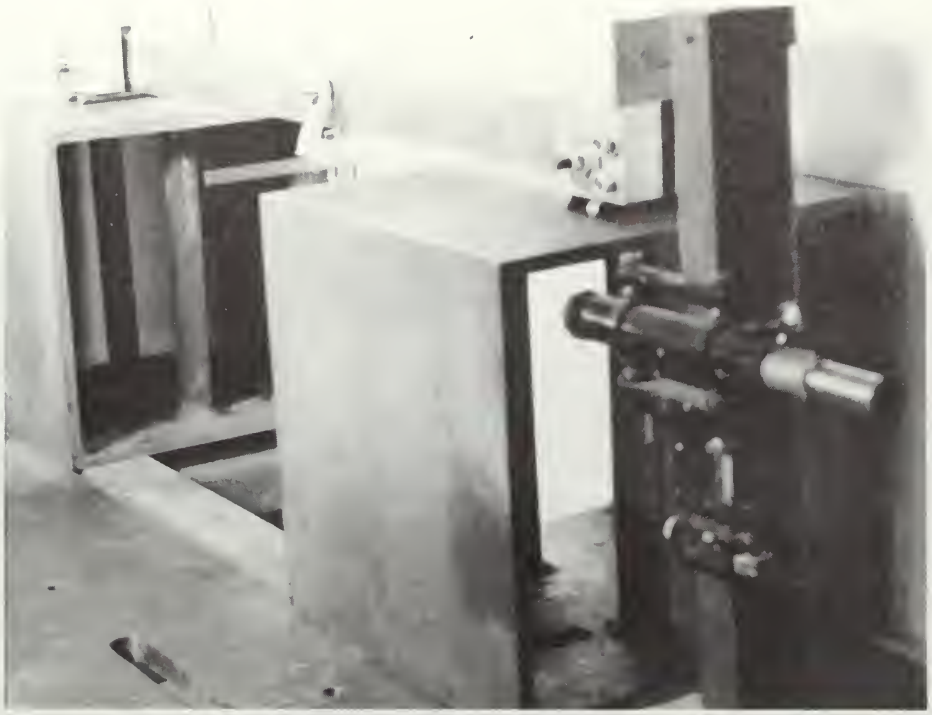

Fig. 4a.

Fig. 4b.

Fig. 4. Close Up Views of Small Deflection Apparatus Showing End Supports, Loading Device and Method of Measuring Centroid Deflections

Fig. 5a.

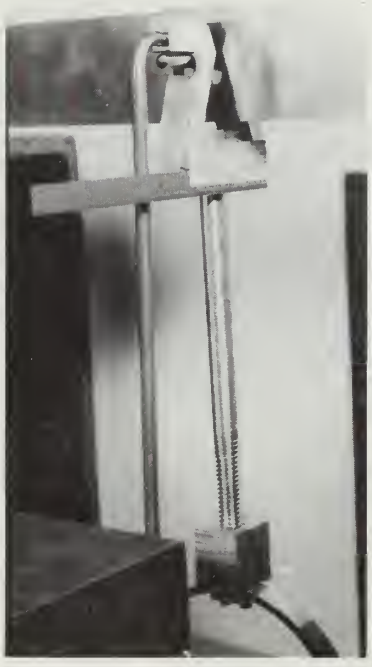

Fig. 5b.

Fig. 5. Views of Small Deflection Apparatus Showing Device Used to Impose Elastic Restraint at Centroid

Fig. 6a. Beam Buckled in First Mode (Spring Constant = 0.0 lb/in)

Fig. 6b. Beam Buckled in Combination of First and Second Modes (Spring Constant = 20 lb/in)

Fig. 6c. Beam Buckled in Second Mode (Spring Constant = 50.5 lb/in)

Fig. 7a. Apparatus Used for Large Deflection Tests of Lateral Instability of Deep Beam

Fig. 7b. First Mode Large Deflection Shape of Deep Beam

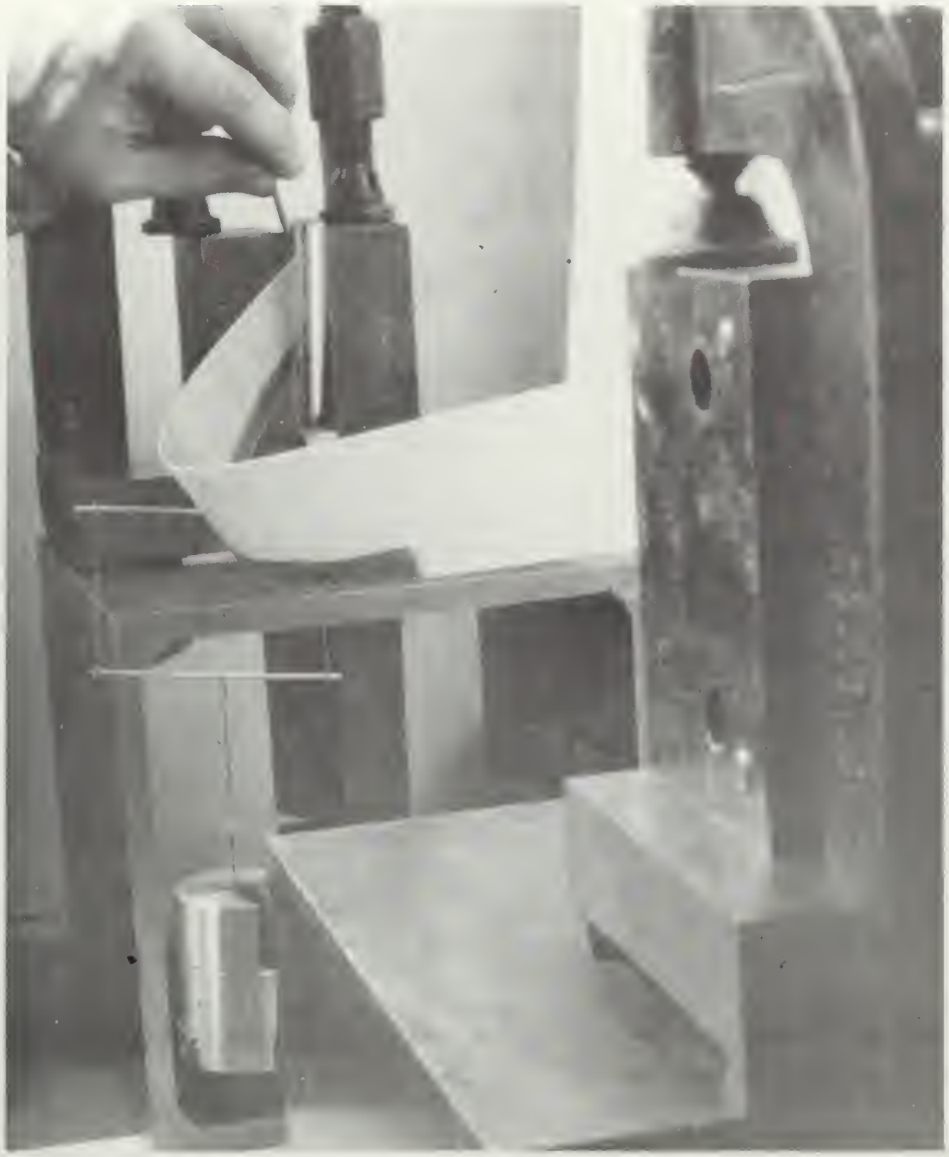

Fig. 7c. Vibrating the End Supports to Achieve Equilibrium in Large Deflection Tests

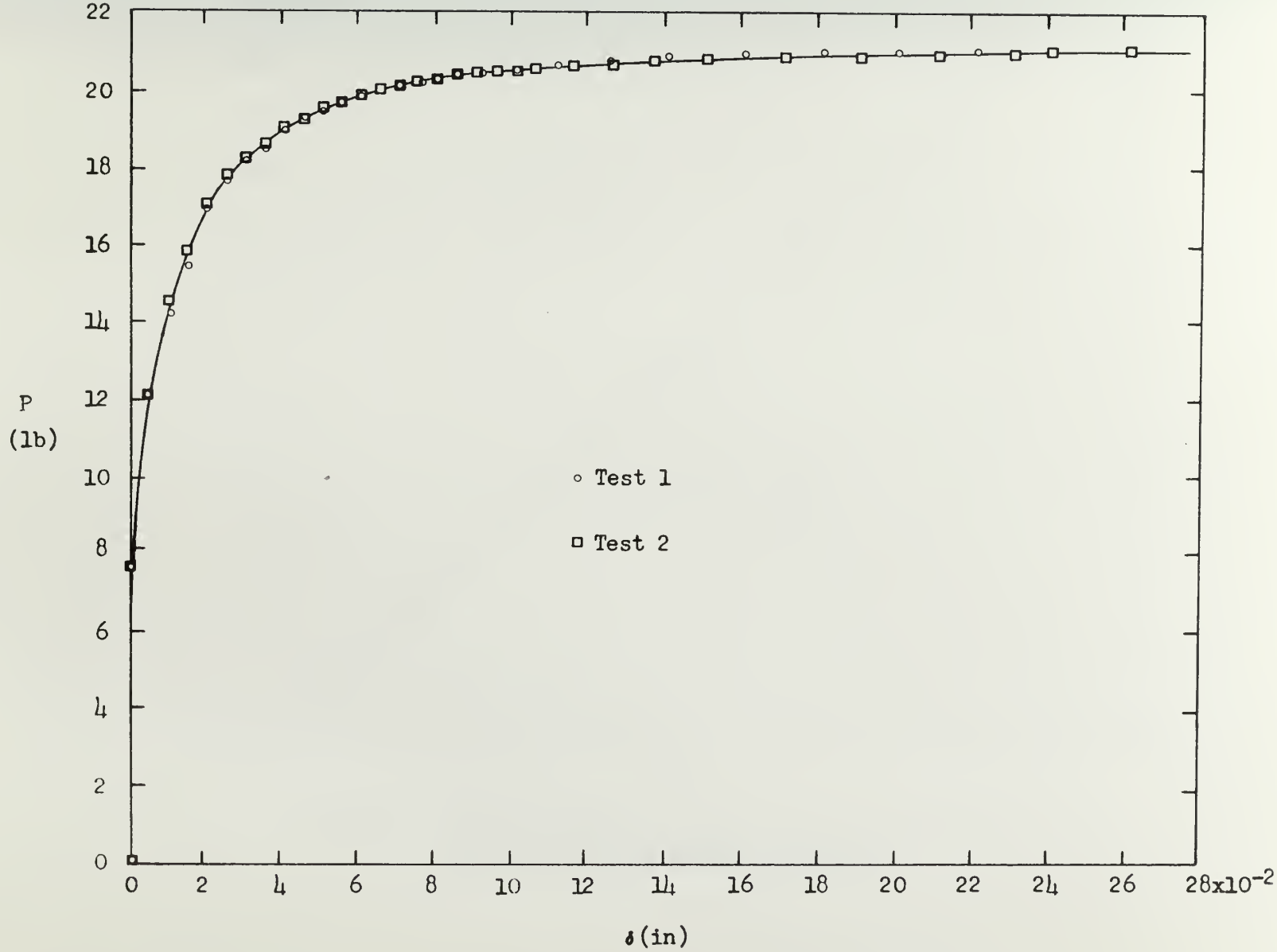

Fig. 8a. Load-Deflection Curves for Small Deflection Tests of Deep Beam With No Elastic Restraint

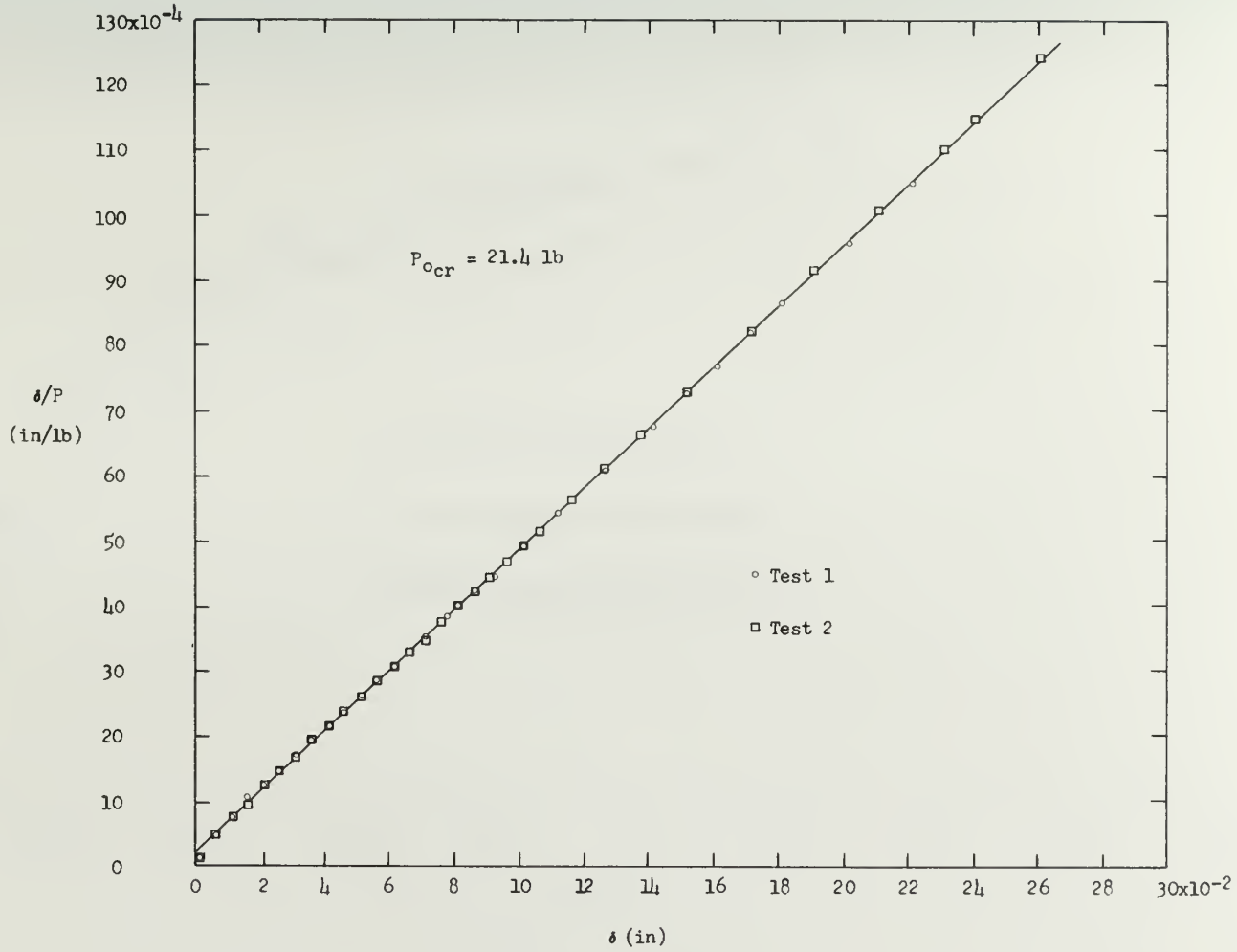

Fig. 8b. Southwell Plots for Small Deflection Tests of Deep Beam With No Elastic Restraint

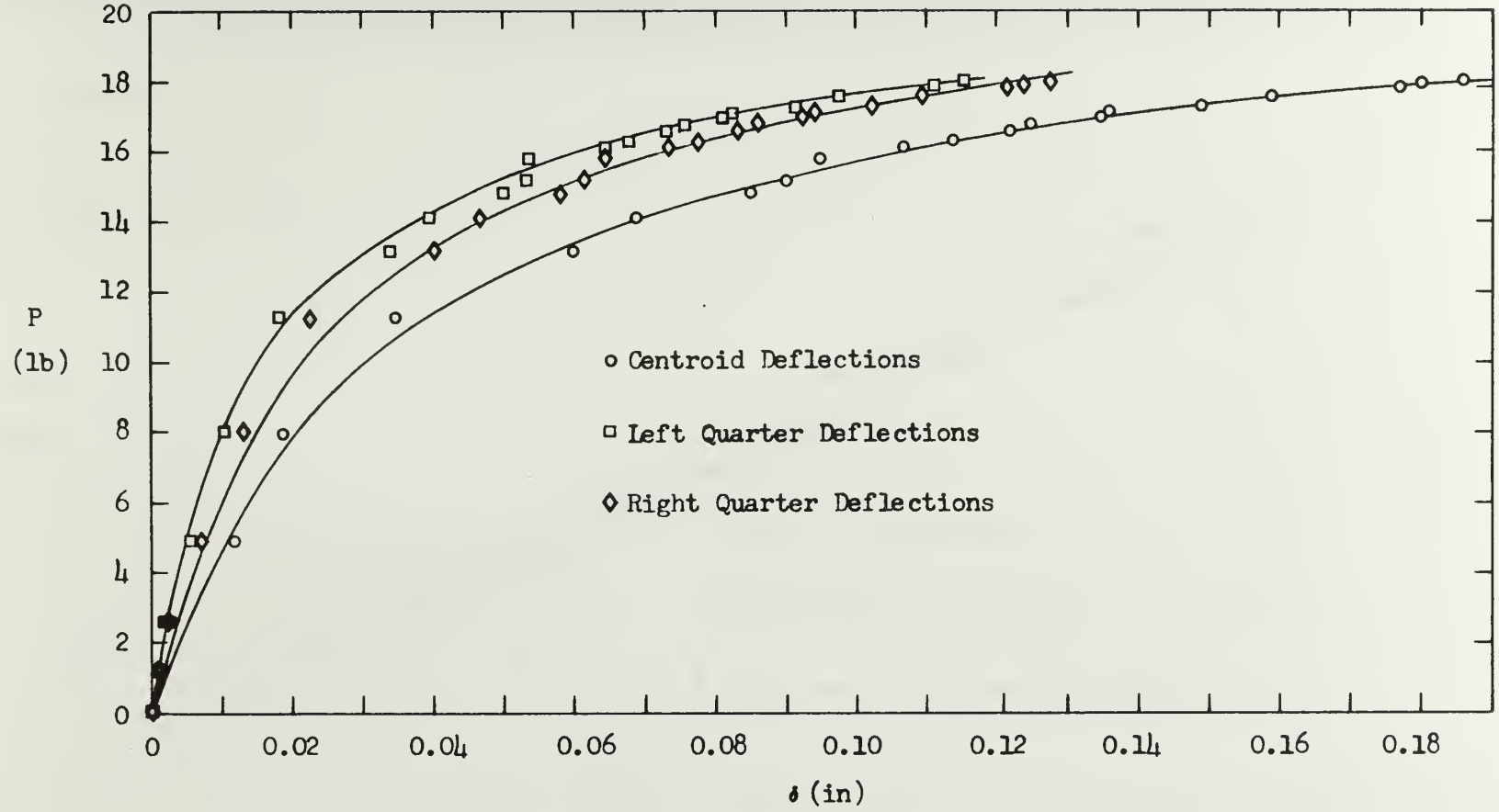

Fig. 9a. Load-Deflection Plots for Small Deflection Tests of Deep Beam (Spring Constant = 0.0 lb/in)

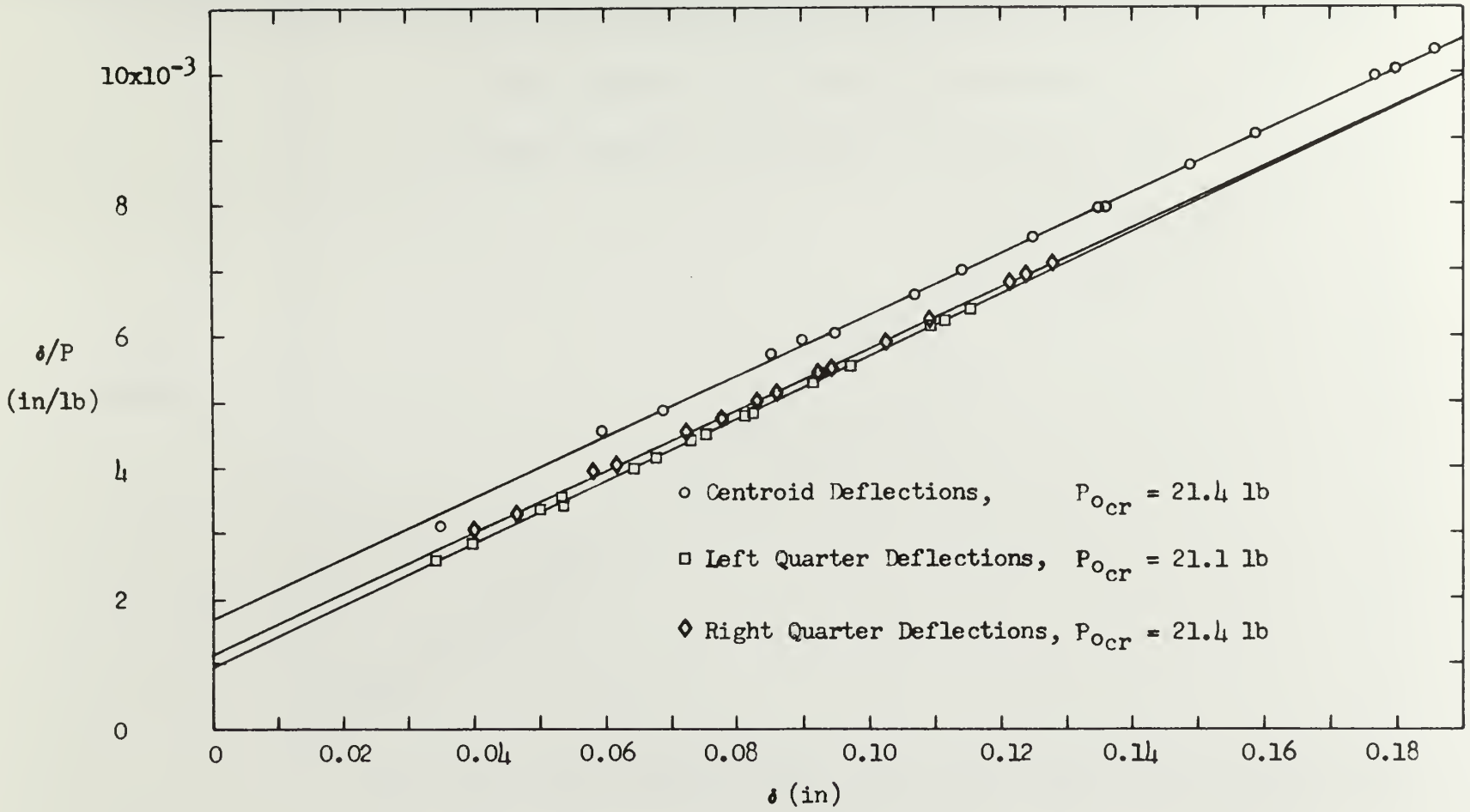

Fig. 9b. Southwell Plots for Small Deflection Tests of Deep Beam (Spring Constant = 0.0 lb/in)

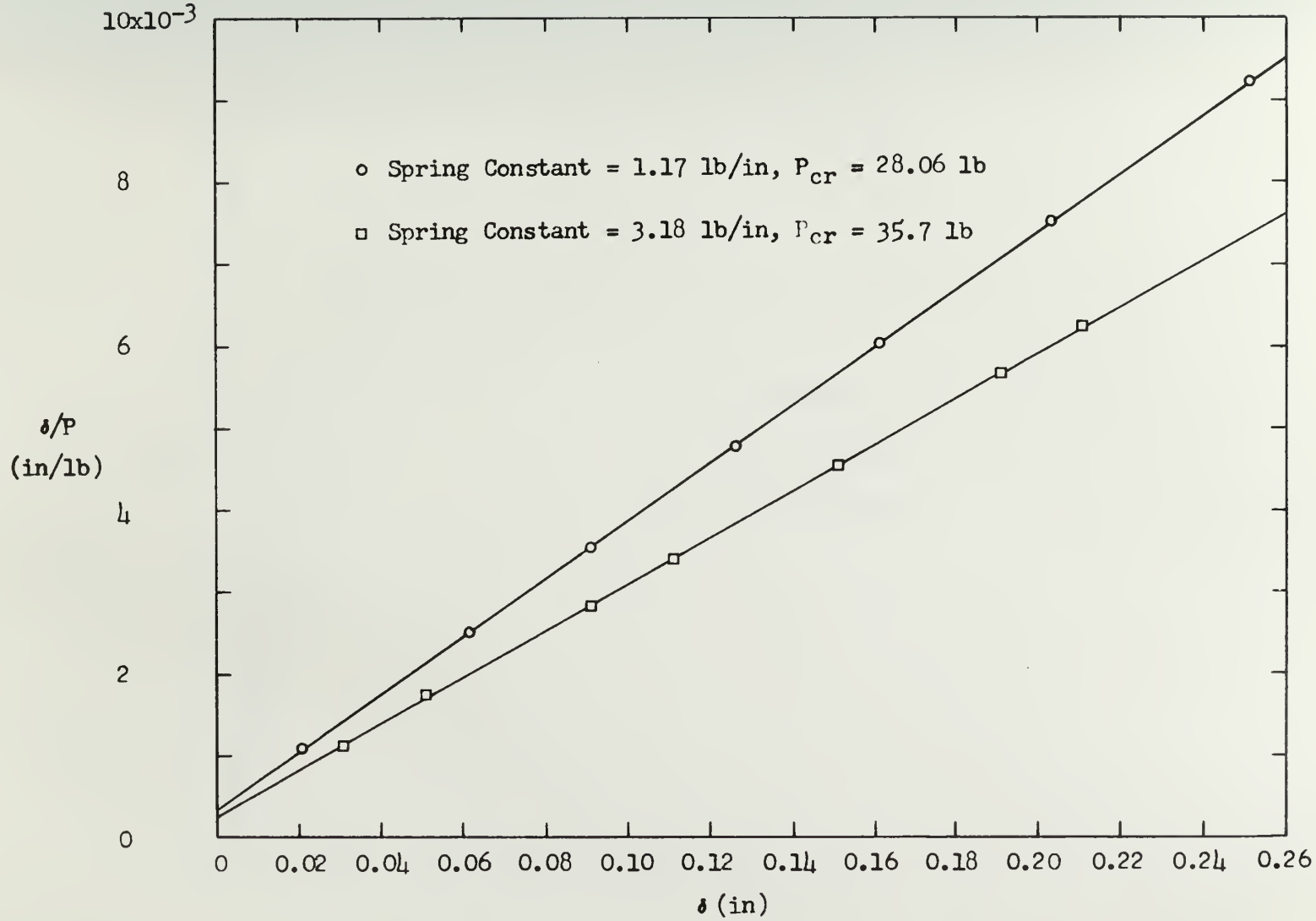

Fig. 9c. Southwell Plots for Small Deflection Tests of Deep Beam
(Spring Constants = 1.17 lb/in and 3.18 lb/in)
(Deflections Measured at Centroid)

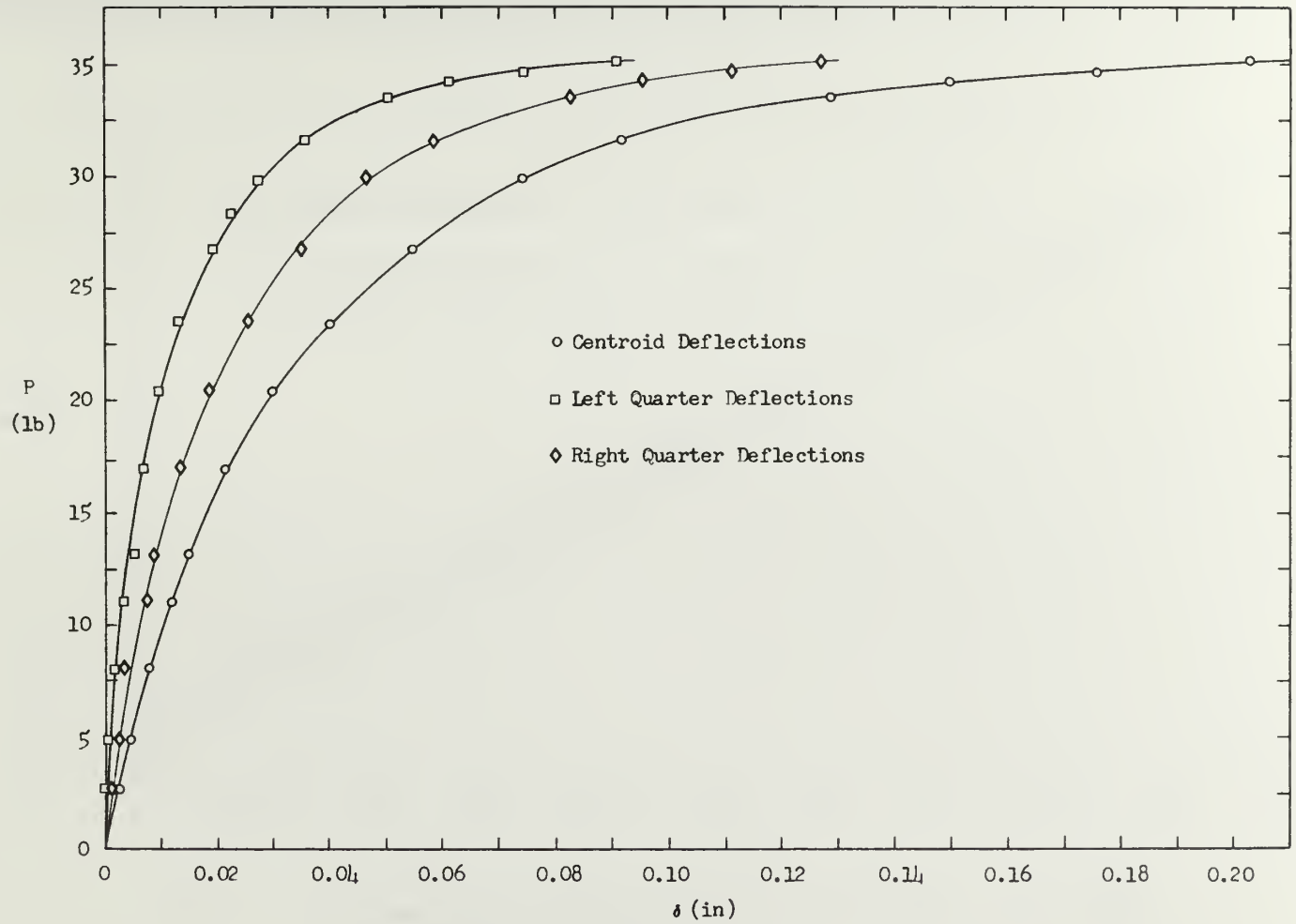

Fig. 9d. Load-Deflection Curves for Small Deflection Tests of Deep Beam (Spring Constant = 4.64 lb/in)

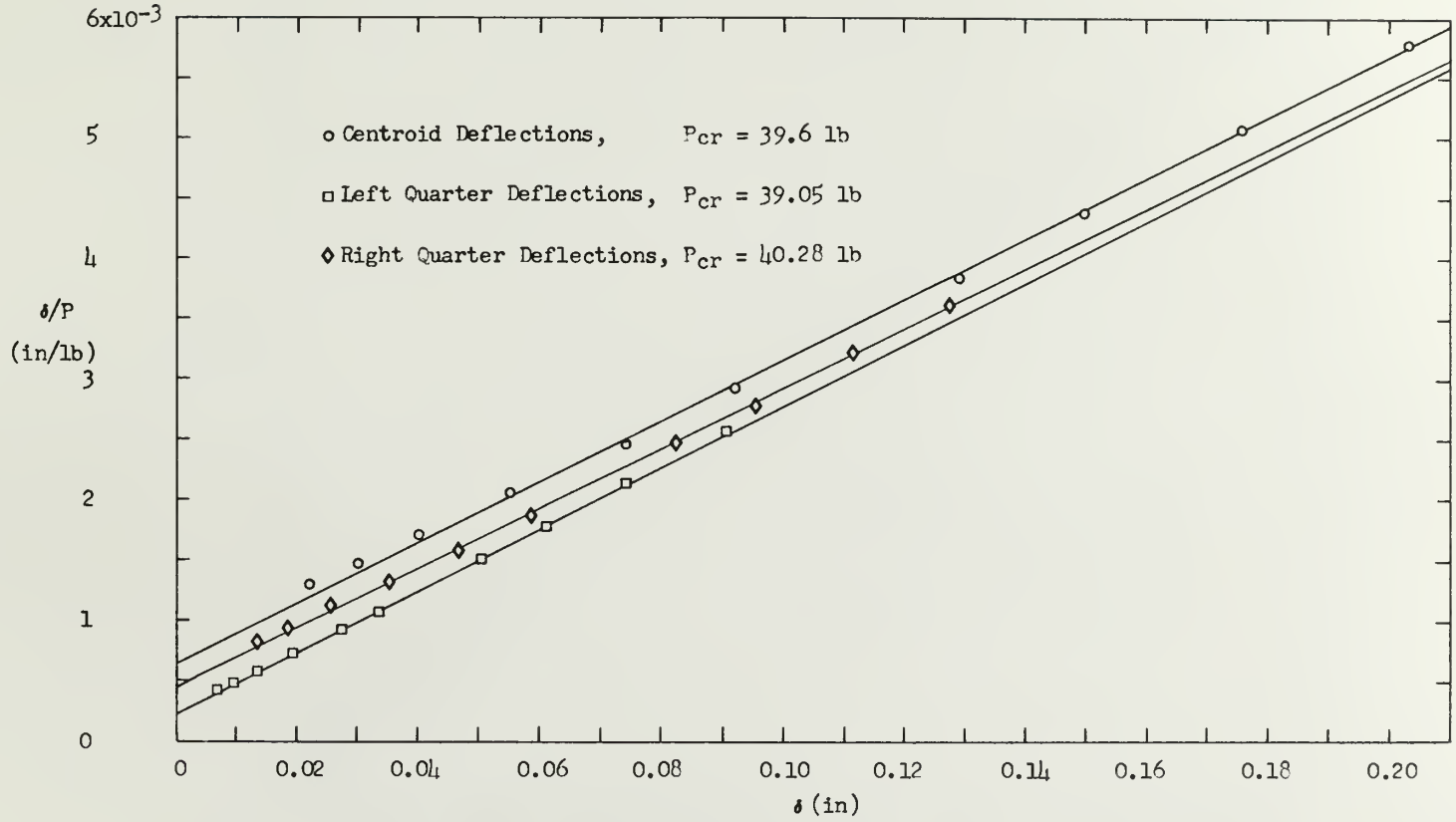

Fig. 9e. Southwell Plots for Small Deflection Tests of Deep Beam (Spring Constant = 4.64 lb/in)

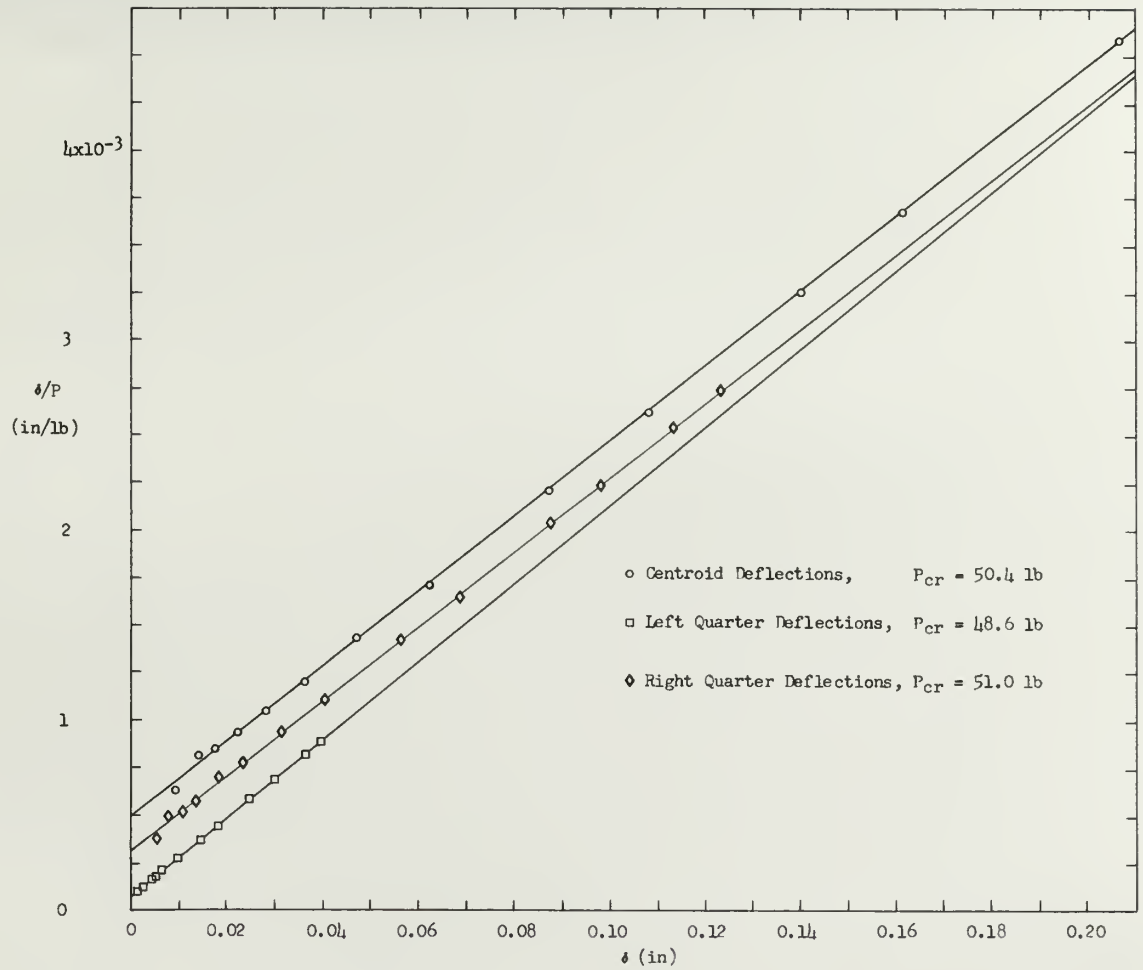

Fig. 9f. Southwell Plots for Small Deflection Tests of Deep Beam (Spring Constant = 9.75 lb/in)

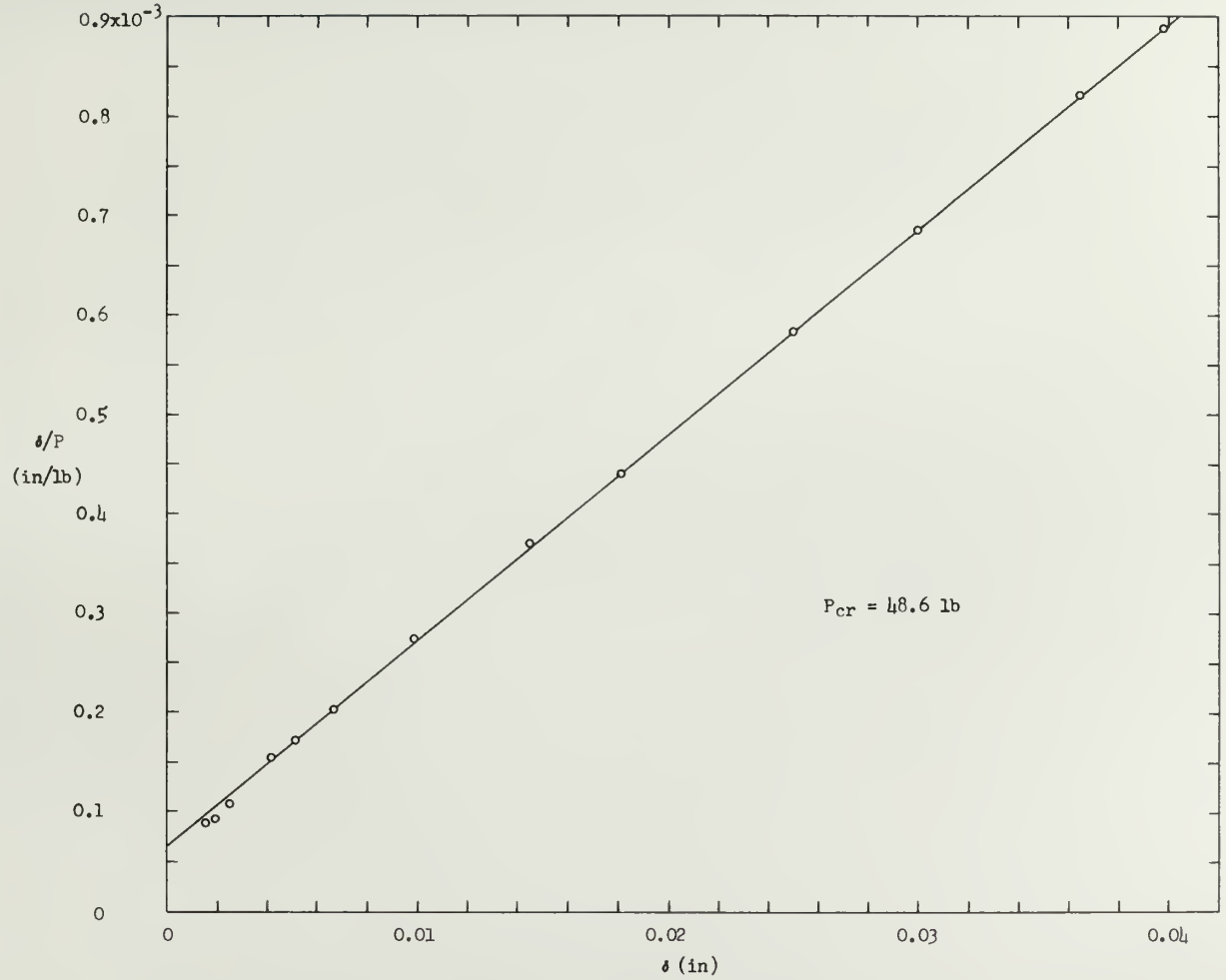

Fig. 9g. Expanded Southwell Plot for Deflections of Left Quarter-Point of Deep Beam (Spring Constant = 9.75 lb/in)

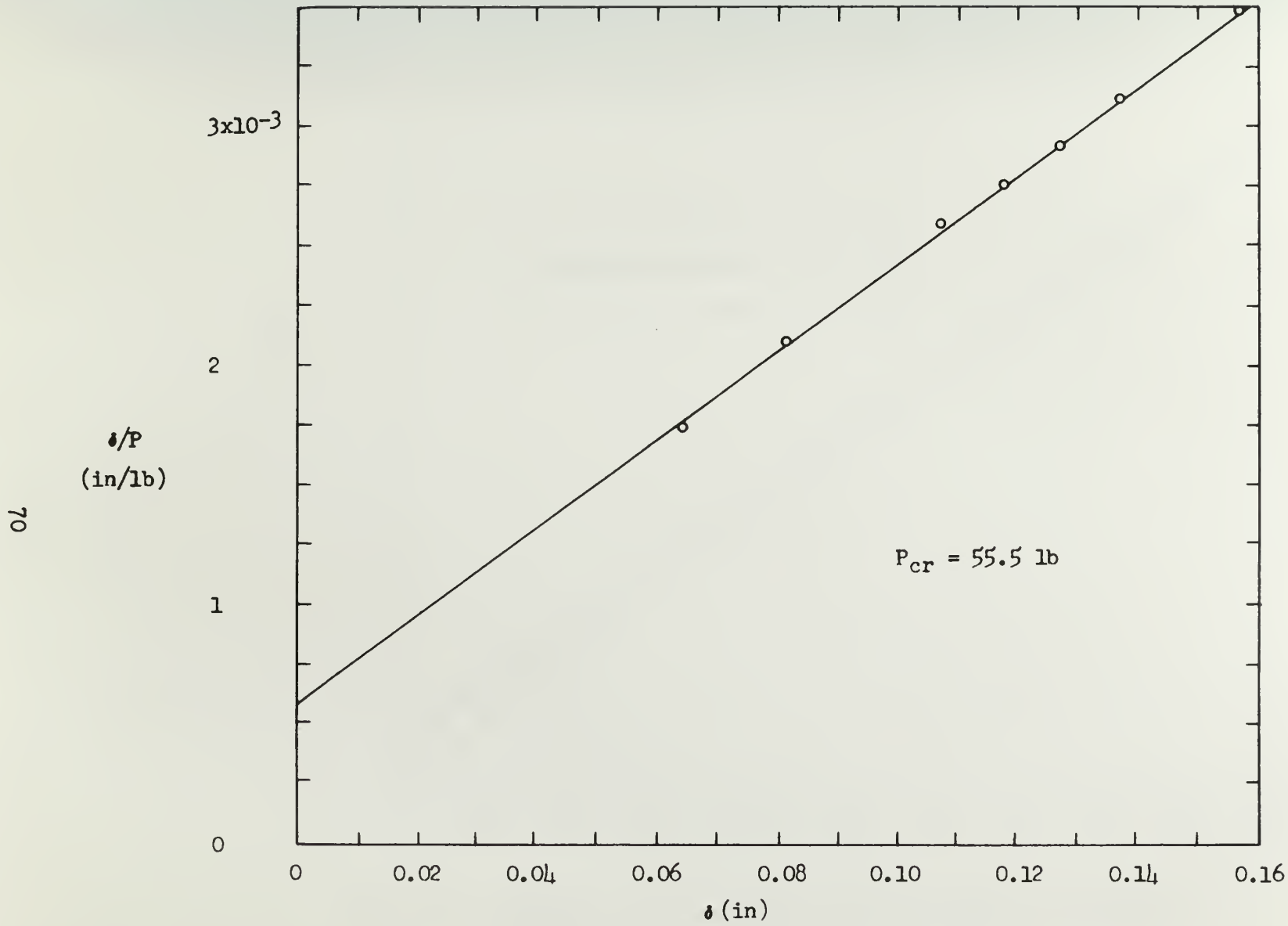

Fig. 9h. Southwell Plot for Small Deflection Tests of Deep Beam
(Deflections Measured at Centroid)
(Spring Constant = 12.5 lb/in)

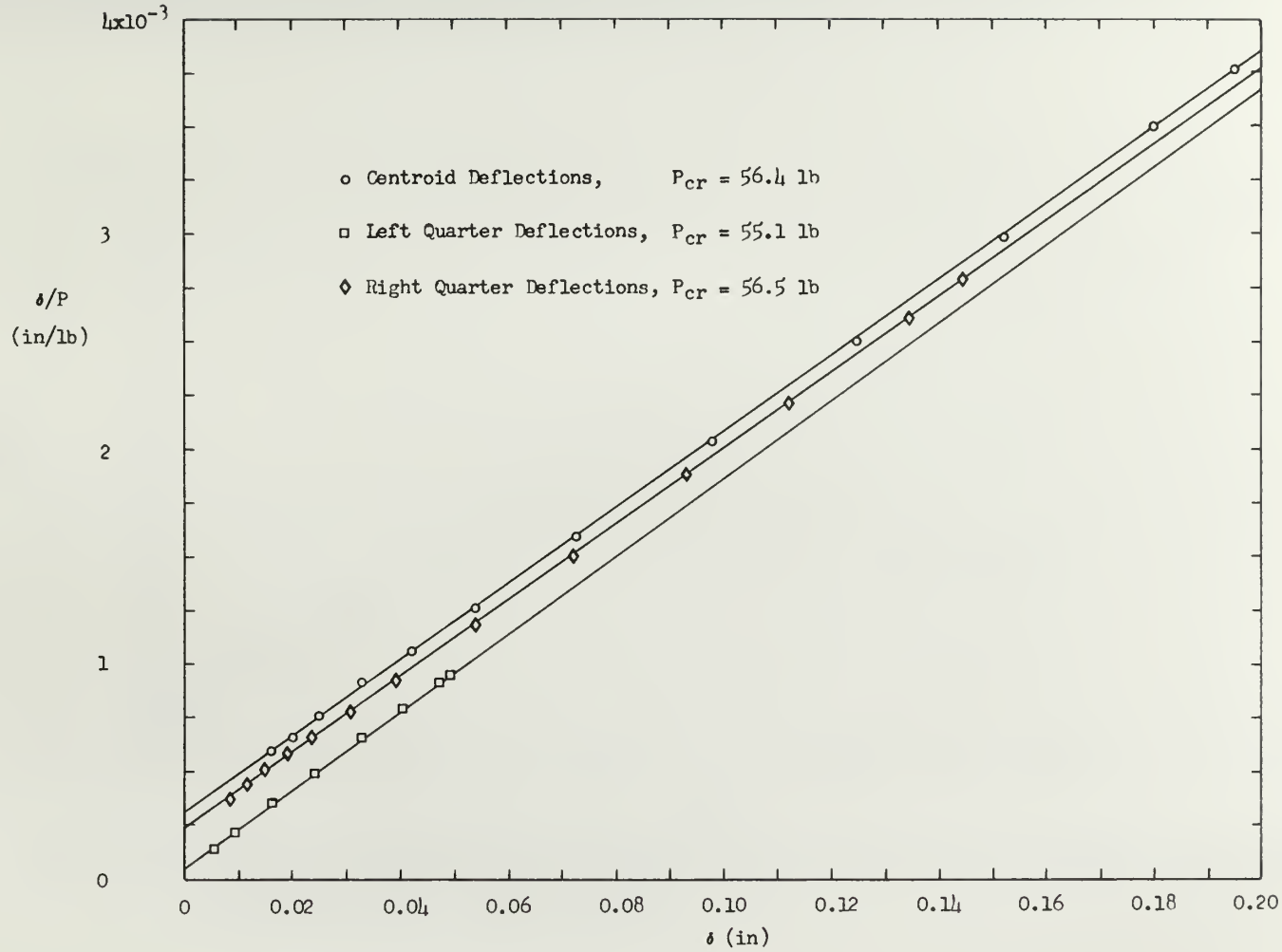

Fig. 9i. Southwell Plots for Small Deflection Tests of Deep Beam (Spring Constant = 15.4 lb/in)

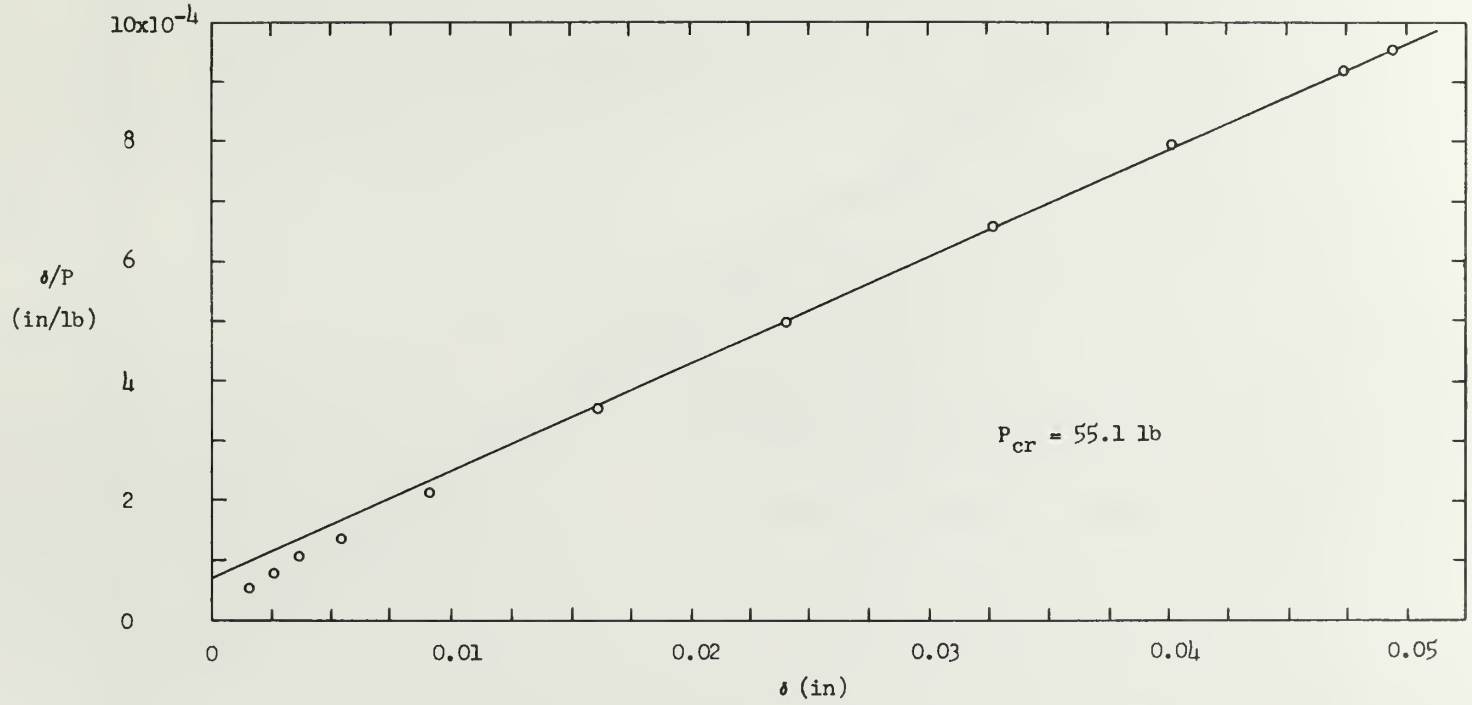

Fig. 9j. Expanded Southwell Plot for Deflections of Left Quarter-Point of Deep Beam (Spring Constant = 15.4 lb/in)

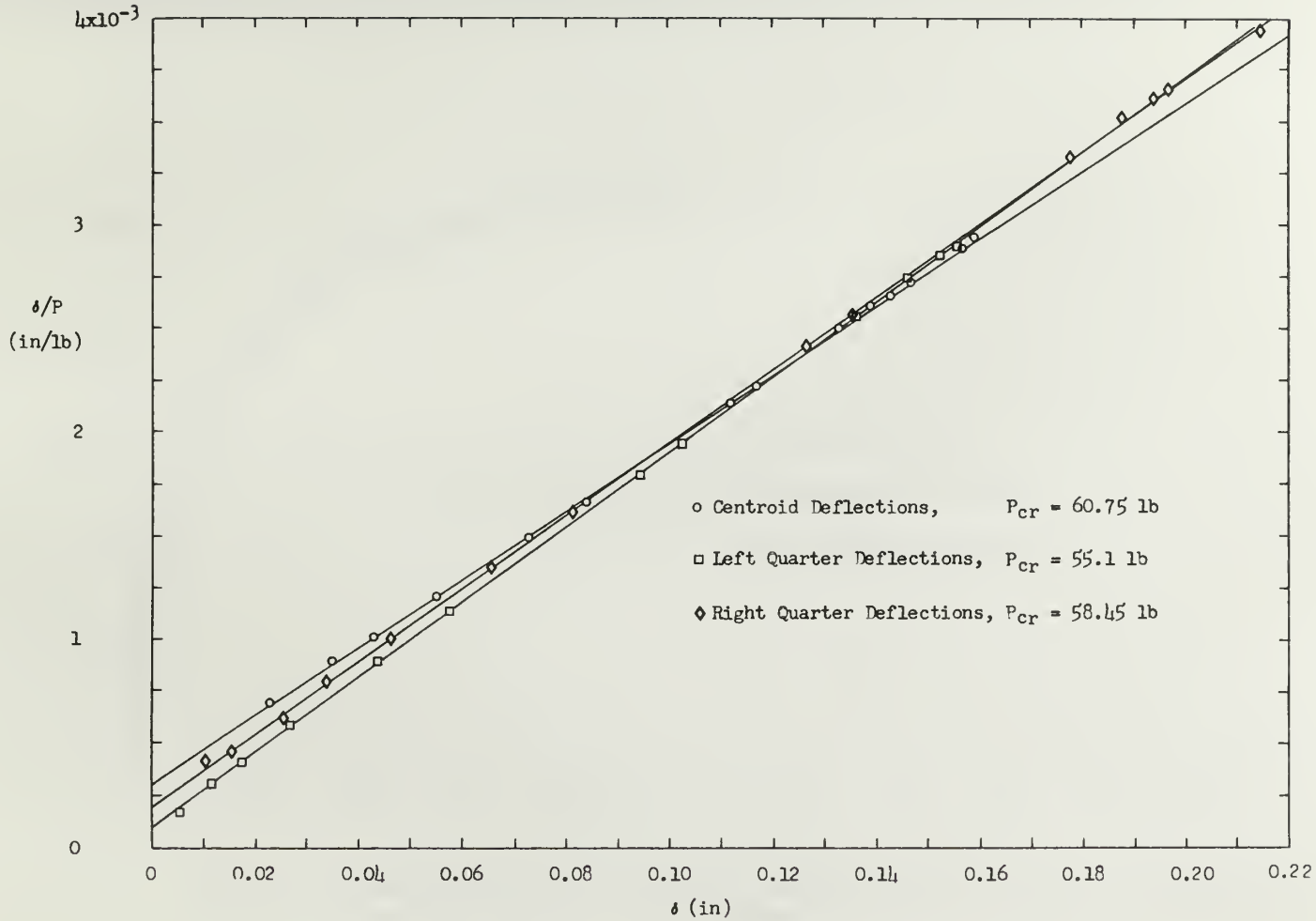

Fig. 9k. Southwell Plots for Small Deflection Tests of Deep Beam (Spring Constant = 20.0 lb/in)

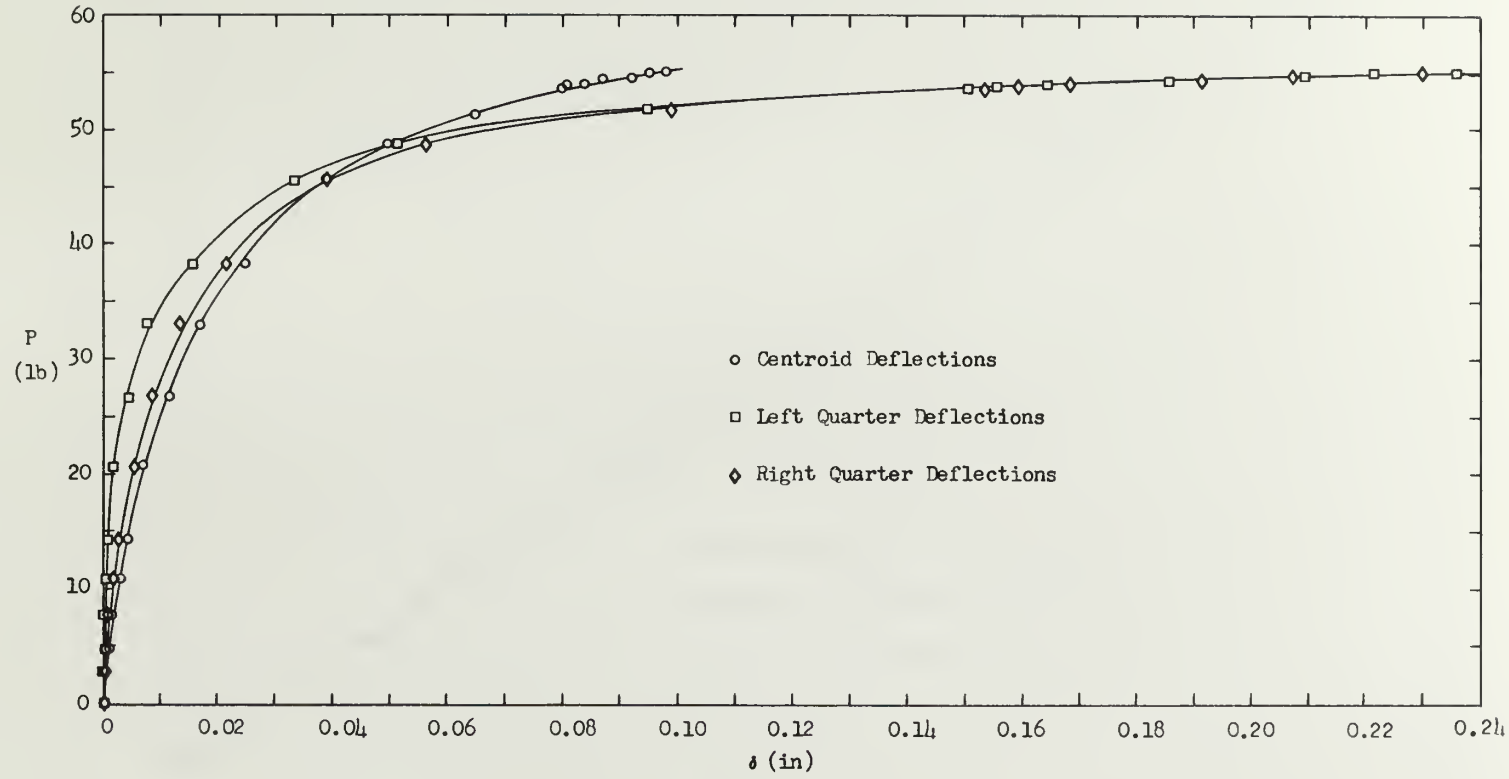

Fig. 91. Load-Deflection Curves for Small Deflection Tests of Deep Beam (Spring Constant = 23.9 lb/in)

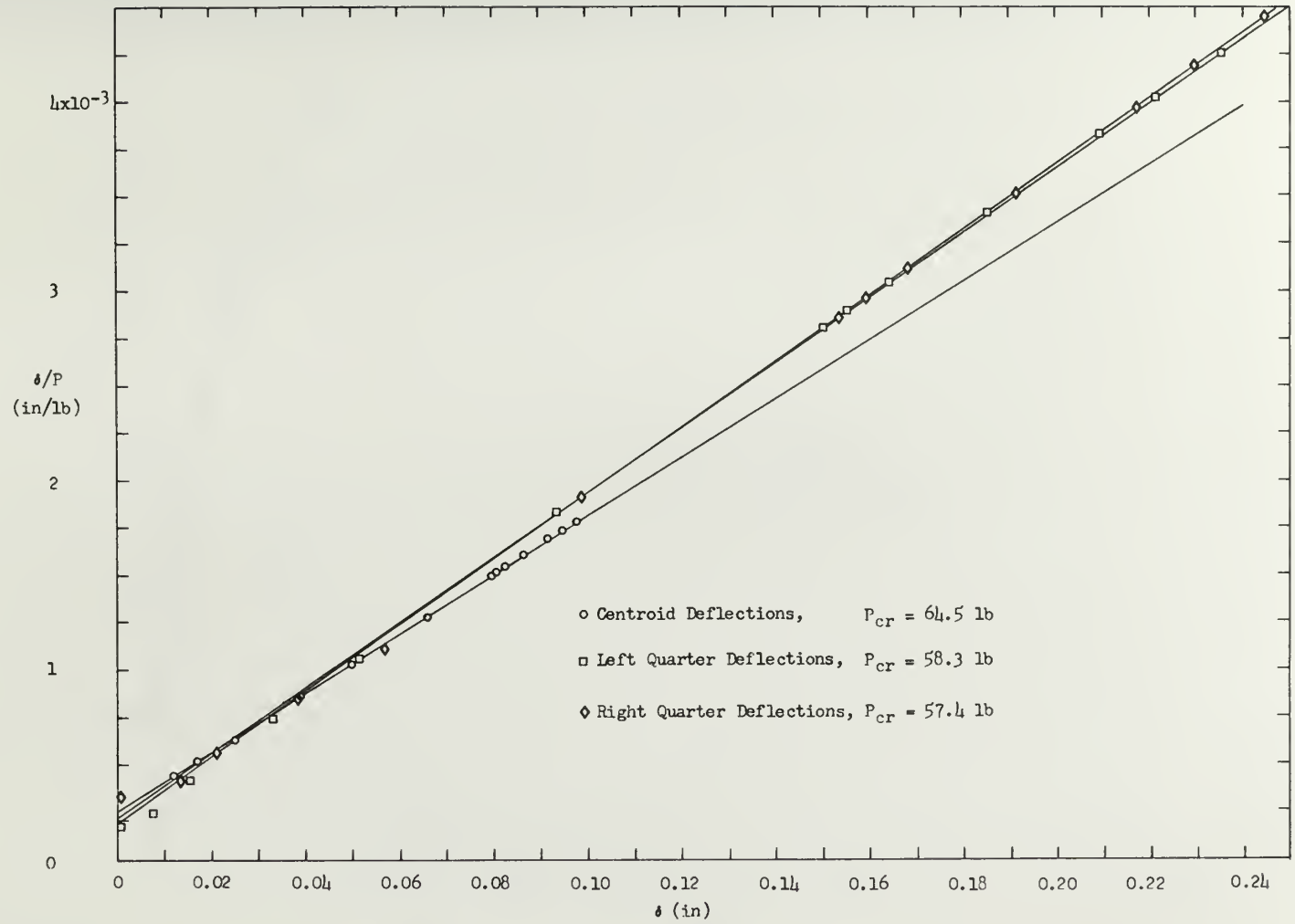

Fig. 9m. Southwell Plots for Small Deflection Tests of Deep Beam (Spring Constant = 23.9 lb/in)

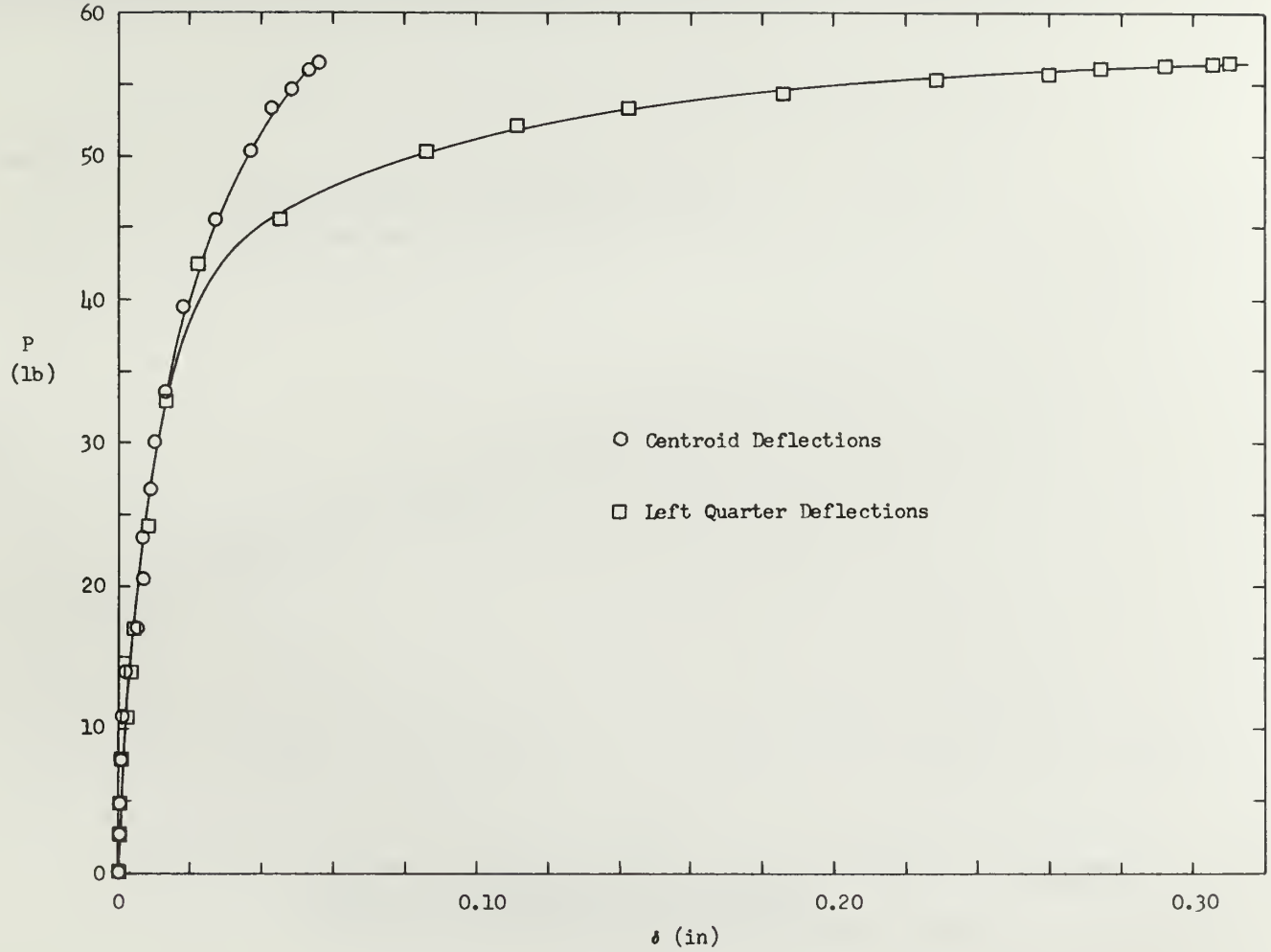

Fig. 9n. Load-Deflection Curves for Small Deflection Tests of Deep Beam (Spring Constant = 34.0 lb/in)

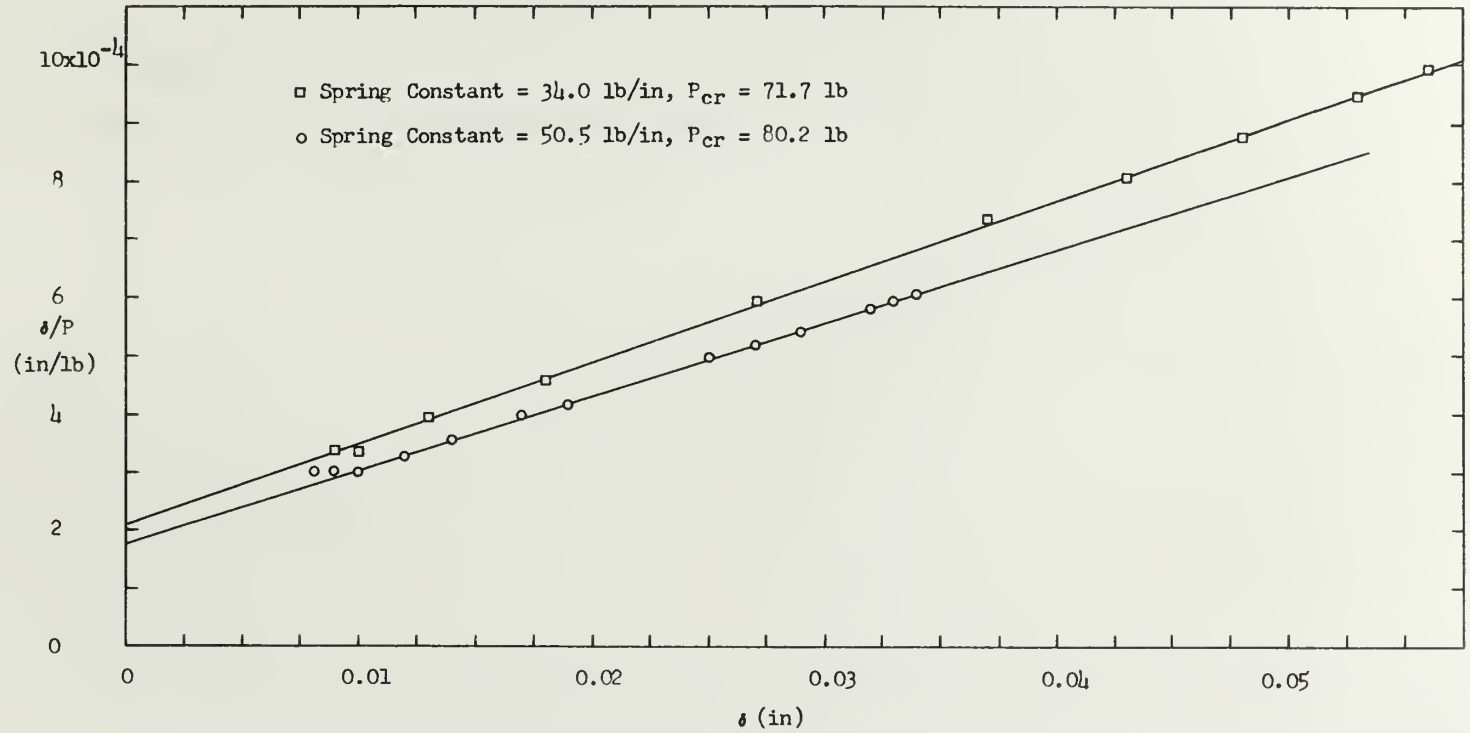

Fig. 9o. Southwell Plots for Small Deflection Tests of Deep Beam
(Deflections Measured at Centroid)
(Spring Constants = 34.0 lb/in and 50.5 lb/in)

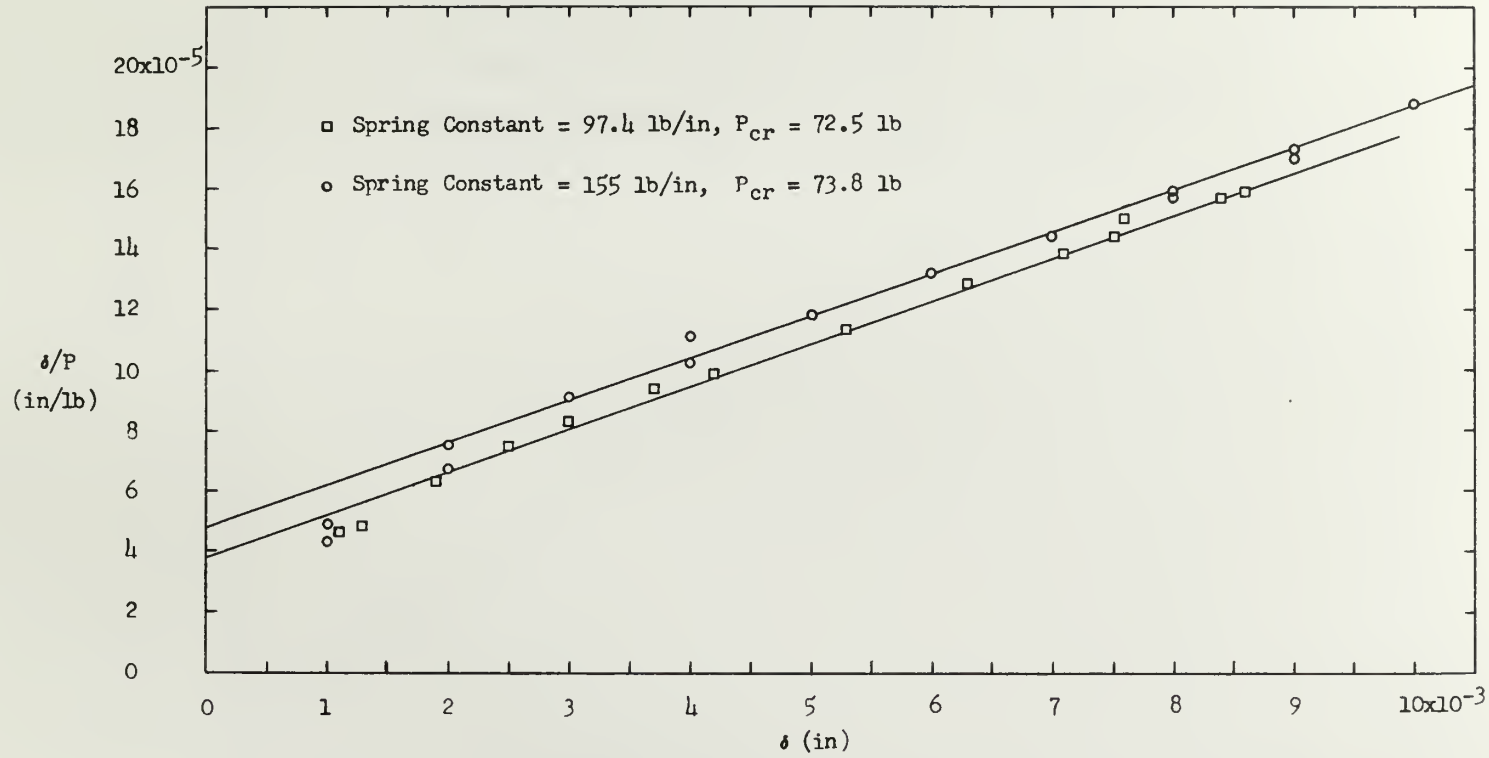

Fig. 9p. Southwell Plots for Small Deflection Tests of Deep Beam
(Deflections Measured at Centroid)
(Spring Constants = 97.4 lb/in and 155 lb/in)

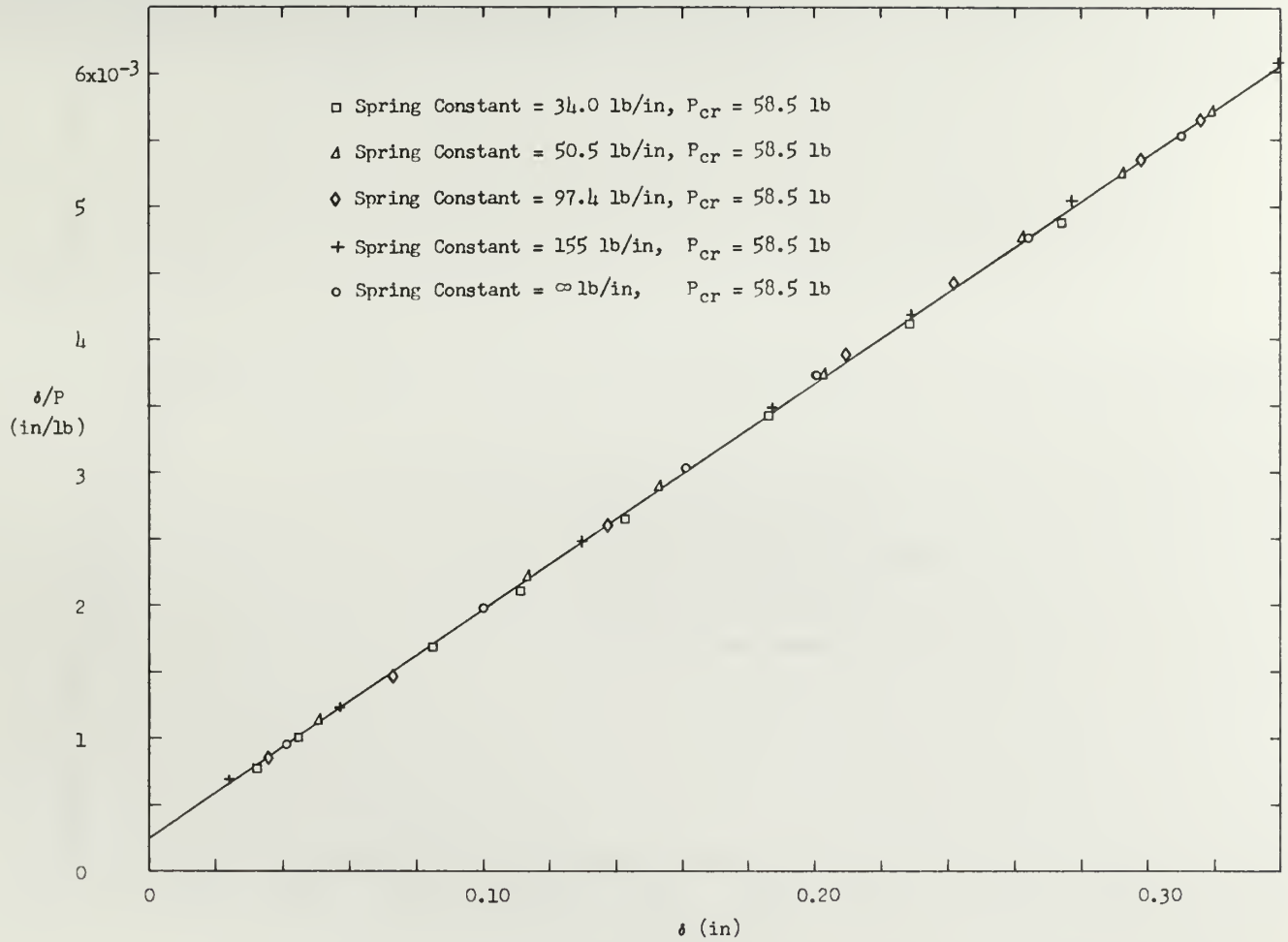

Fig. 9q. Southwell Plots for Small Deflection Tests of Deep Beam (Deflections Measured at Left Quarter) (Spring Constants = 34.0 lb/in, 50.5 lb/in, 97.4 lb/in, 155 lb/in and ∞ lb/in)

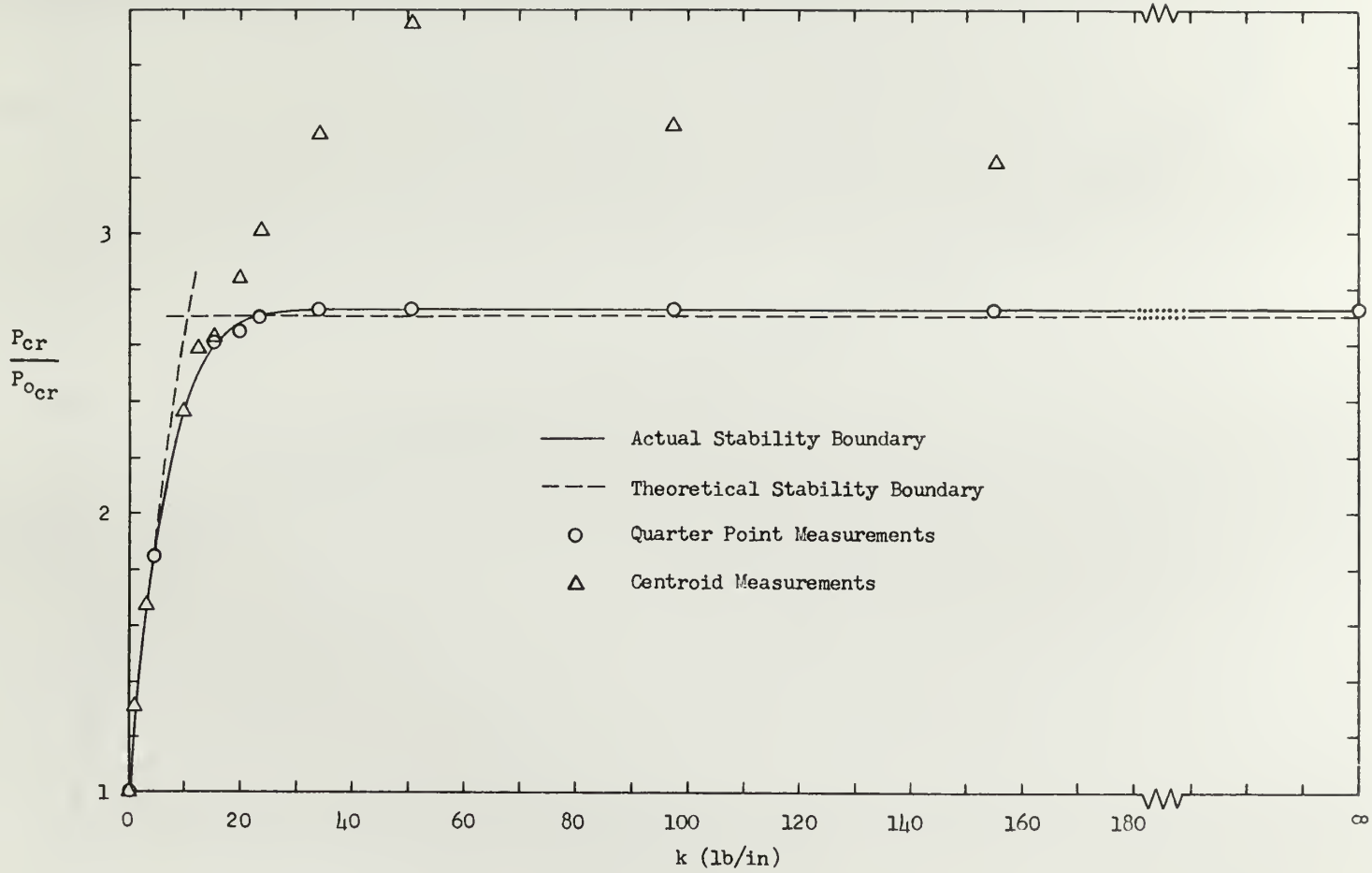

Fig. 9r. Effect on Lateral Buckling Load of Various Elastic Restraints at Centroid of Deep Beam

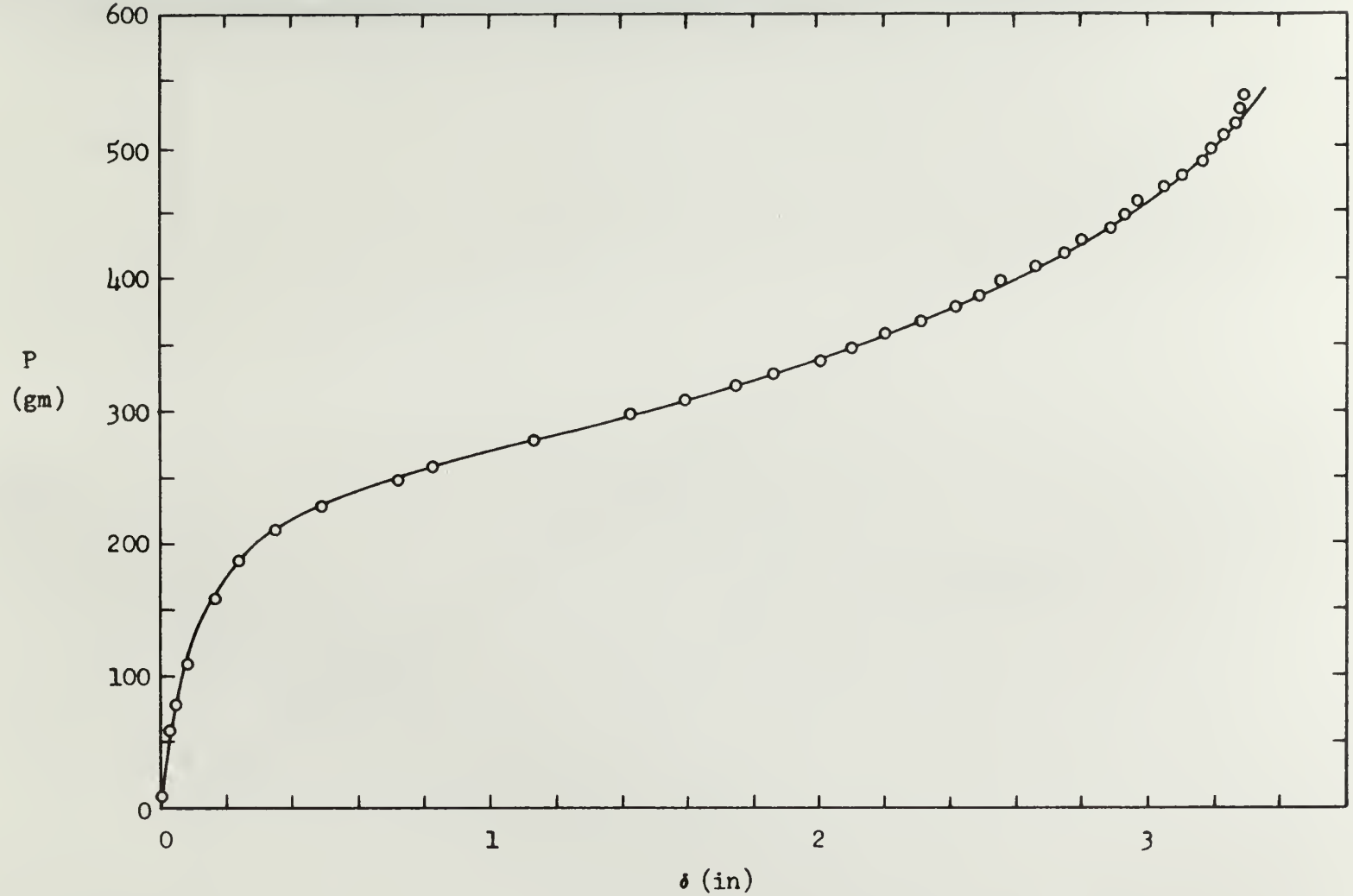

Fig. 10a. Load-Deflection Plot for Fibreglass Beam
(Deflections Measured at Centroid)

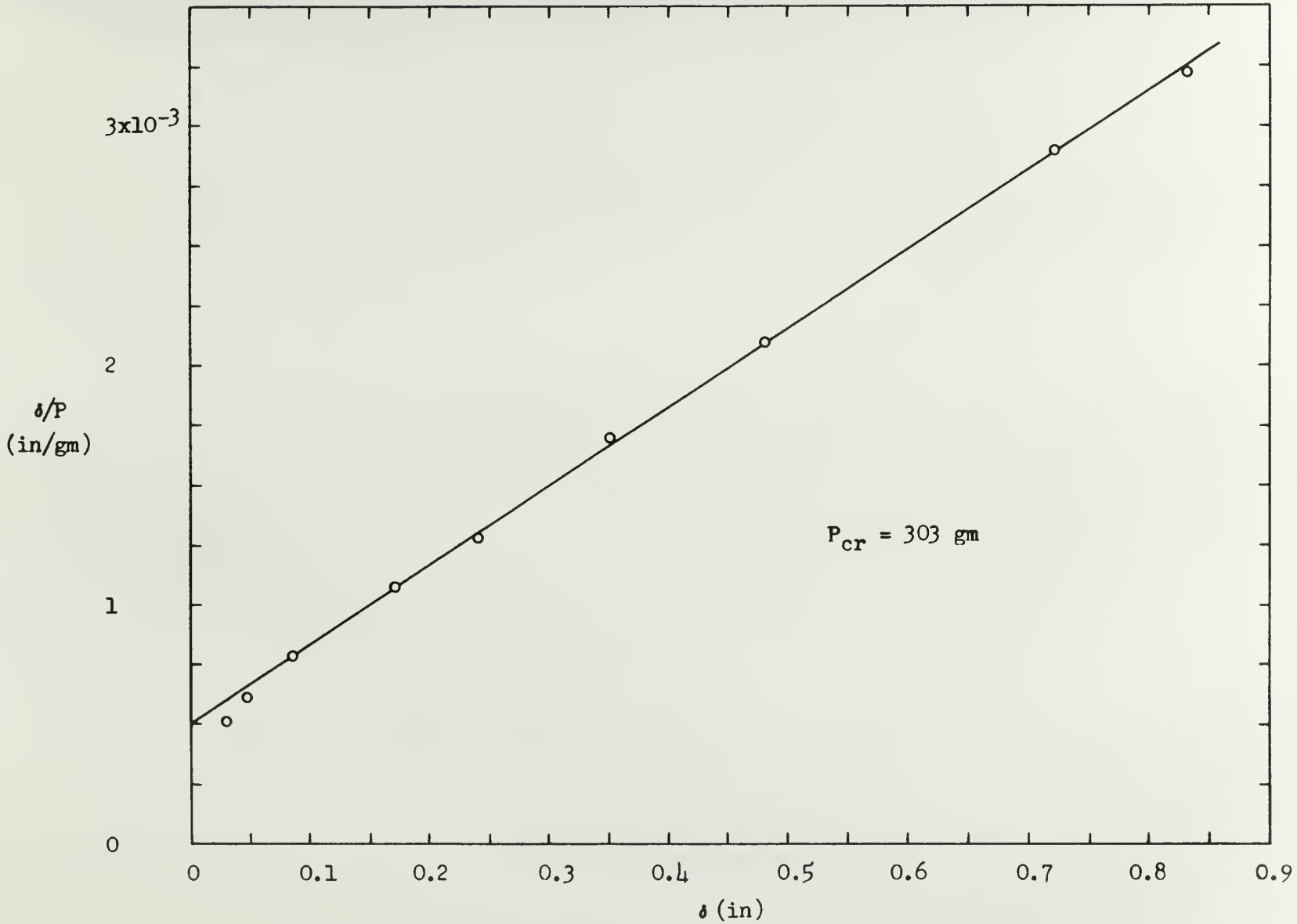

Fig. 10b. Southwell Plot for Fibreglass Beam
(Deflections Measured at Centroid)

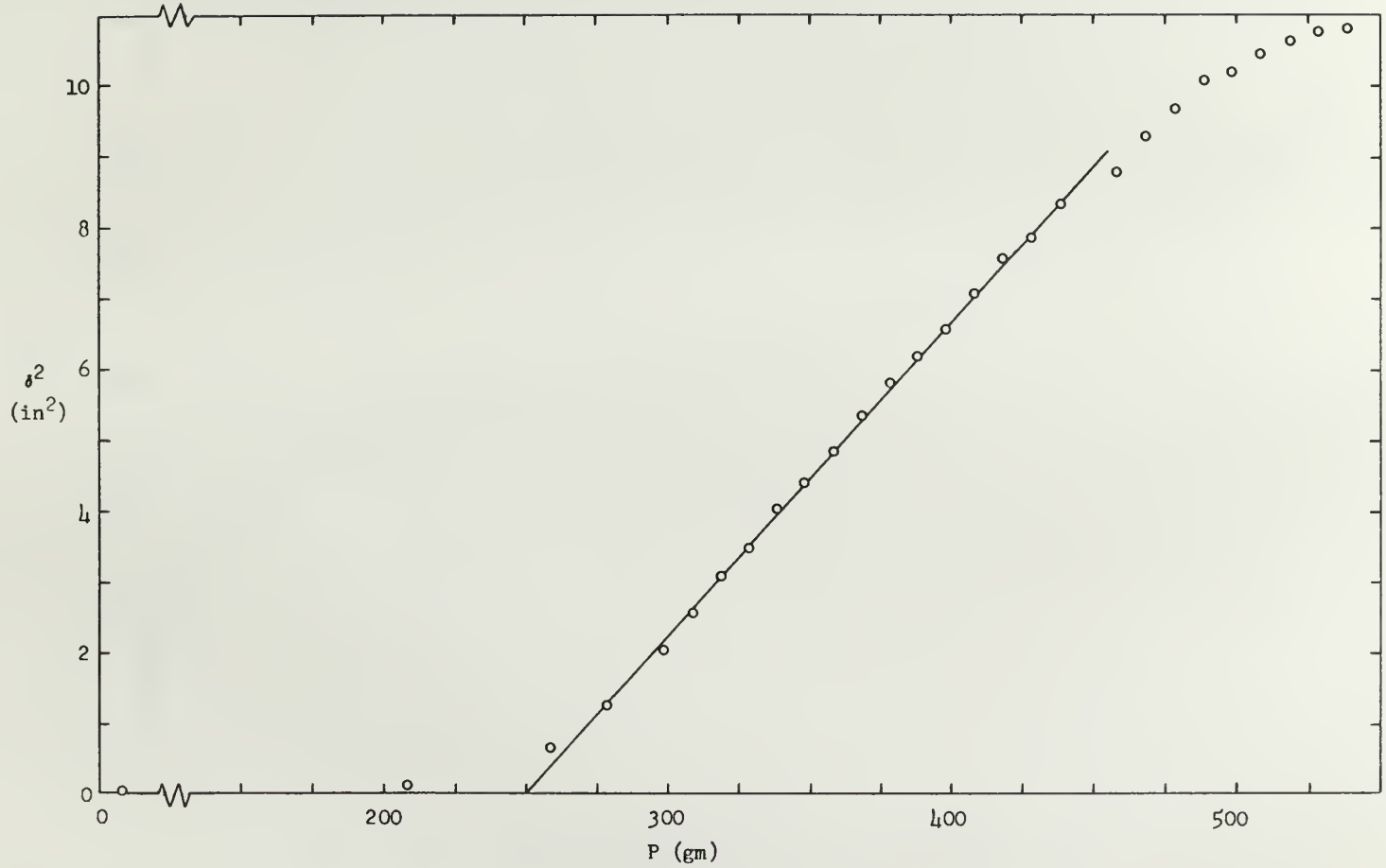

Fig. 10c. Large Deflection Plot for Fibreglass Beam
(Deflections Measured at Centroid)

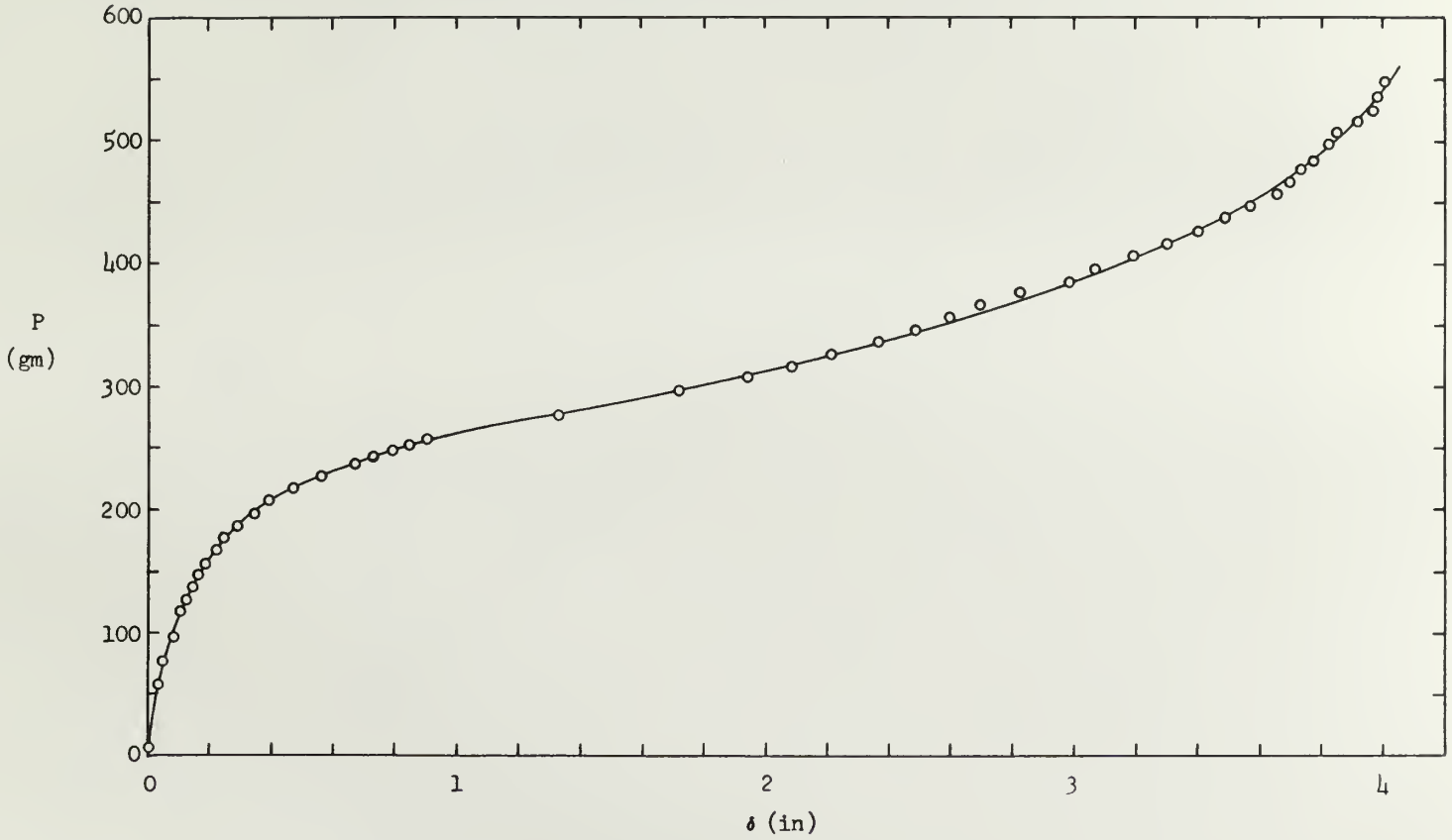

Fig. 10d. Load-Deflection Plot for Fibreglass Beam
(Deflections Measured at Top Fibre)

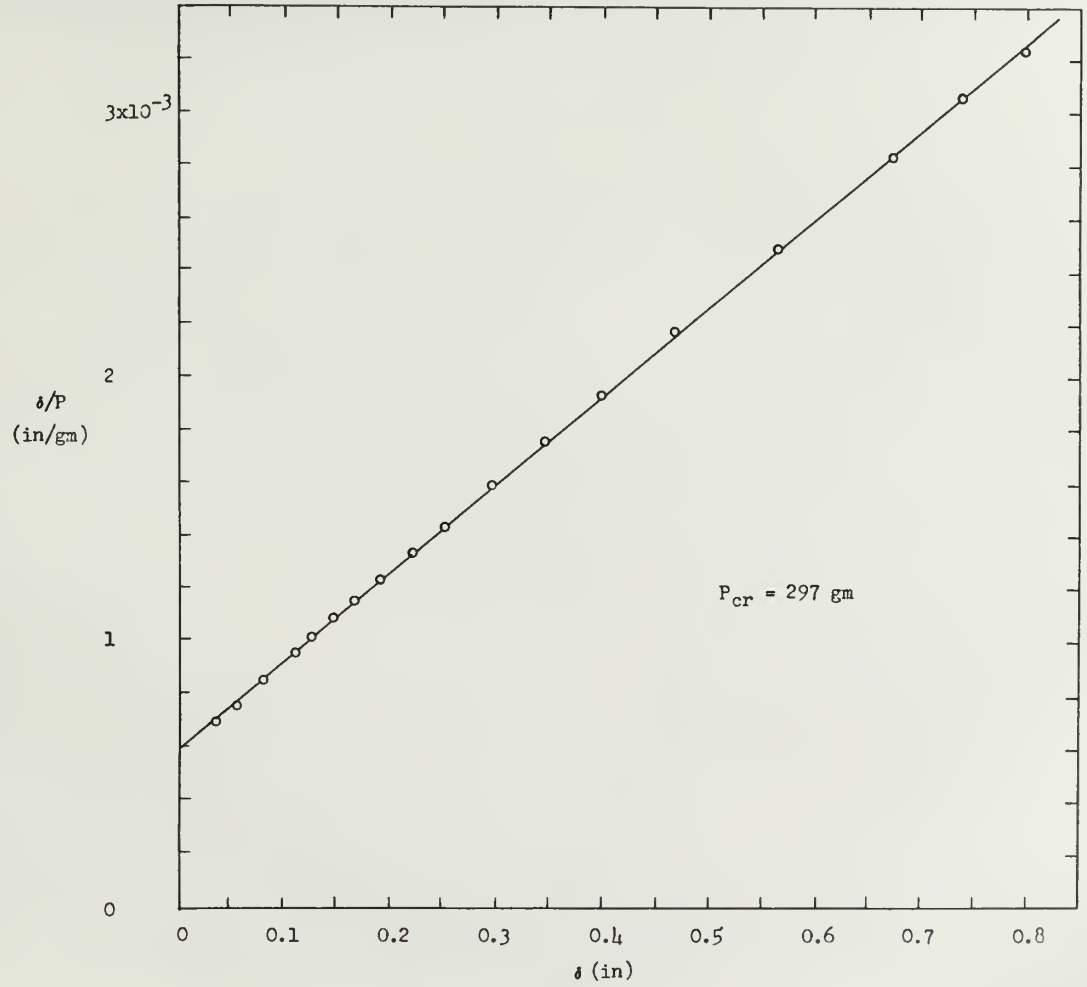

Fig. 10e. Southwell Plot for Fibreglass Beam
(Deflections Measured at Top Fibre)

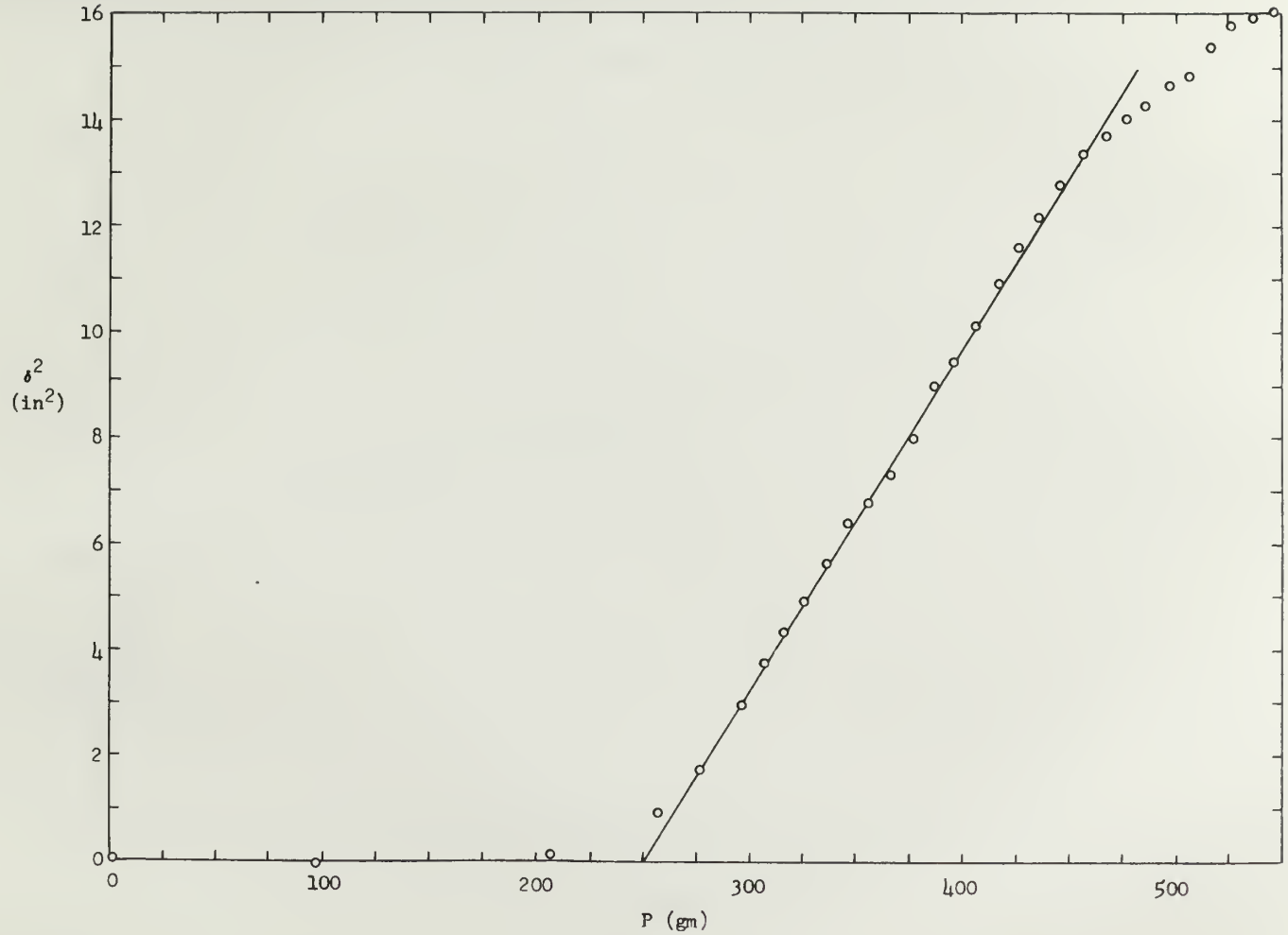

Fig. 10f. Large Deflection Plot for Fibreglass Beam
(Deflections Measured at Top Fibre)

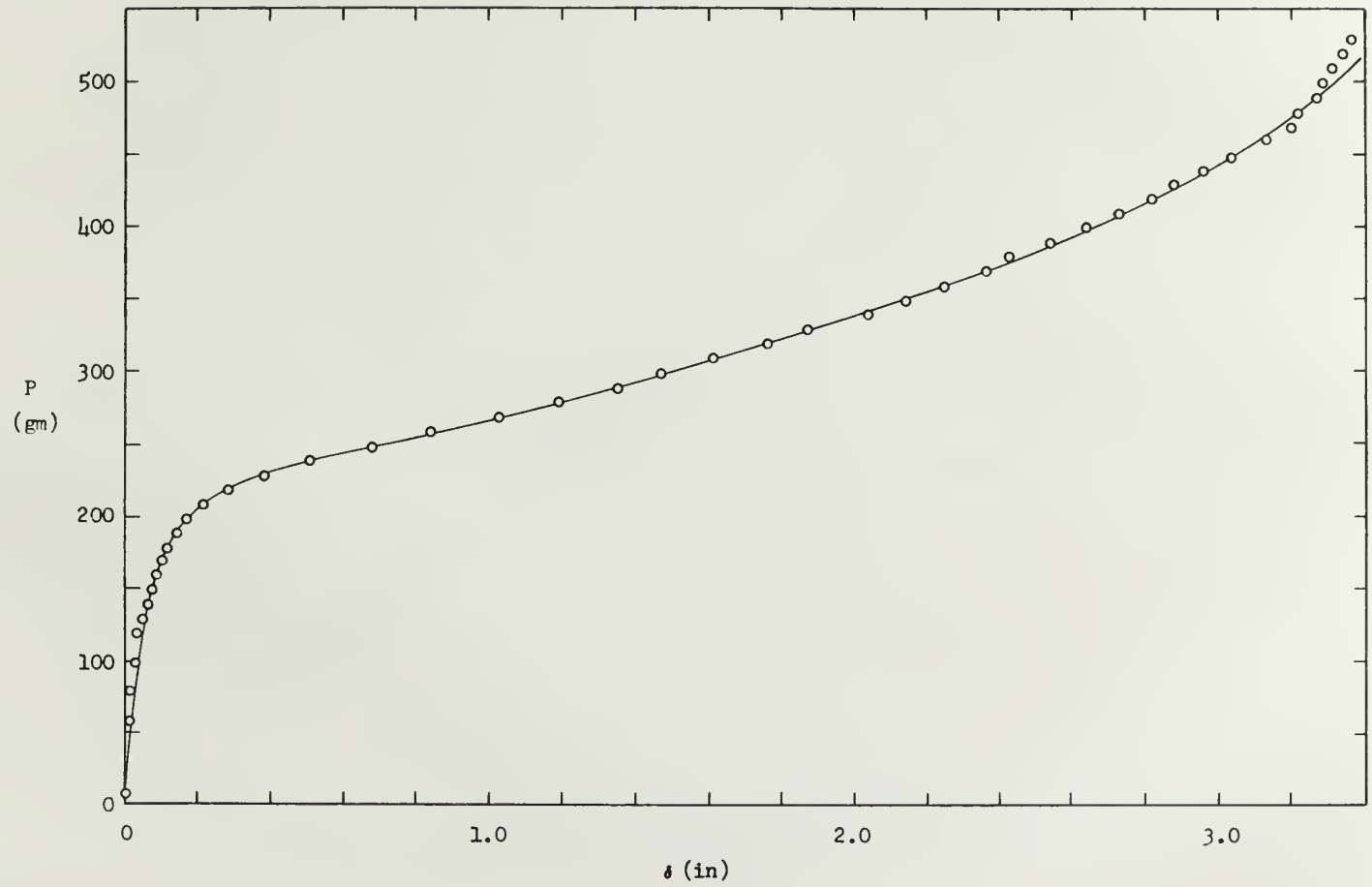

Fig. 11a. Load-Deflection Plot for Spring Steel Beam

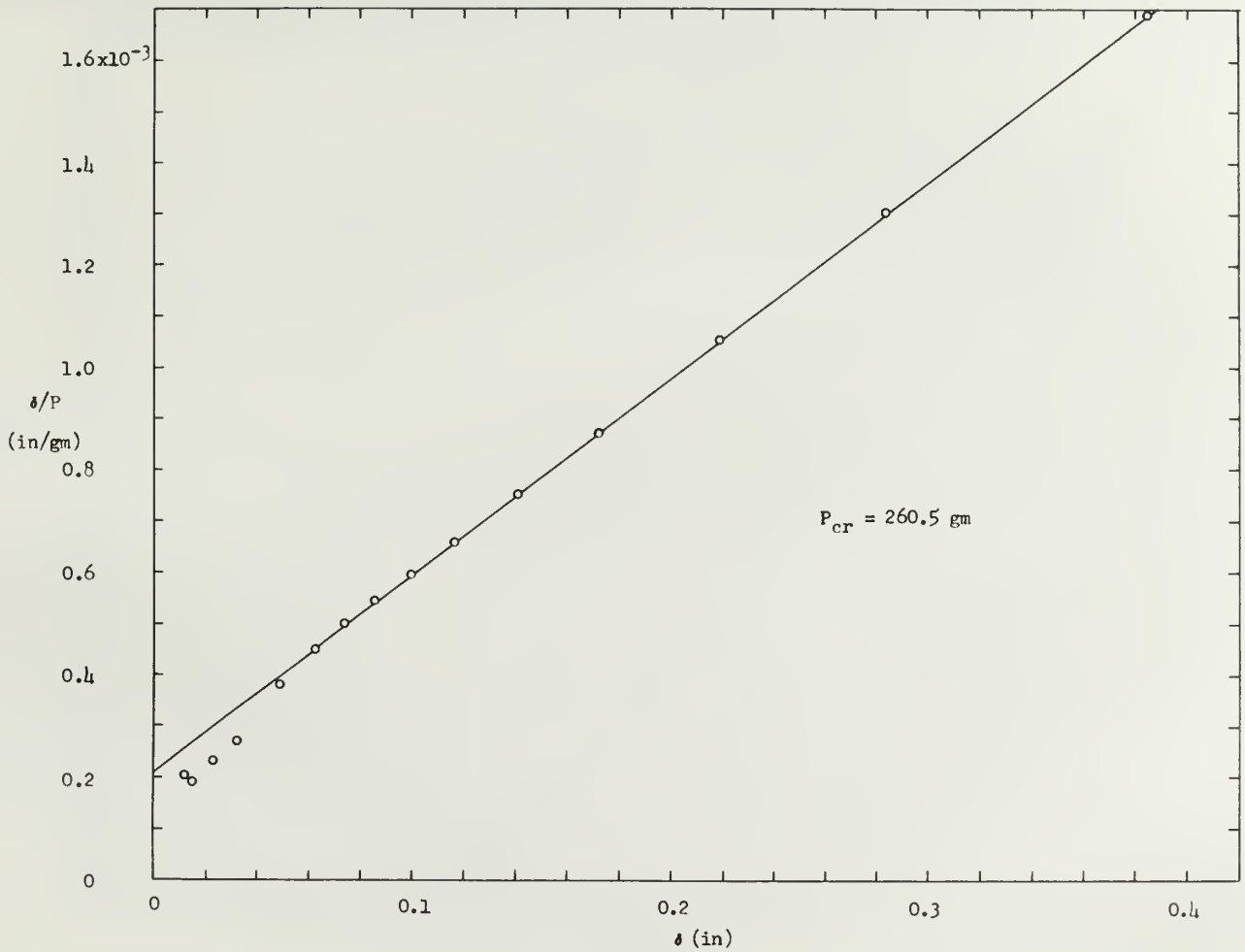

Fig. 11b. Southwell Plot for Spring Steel Beam

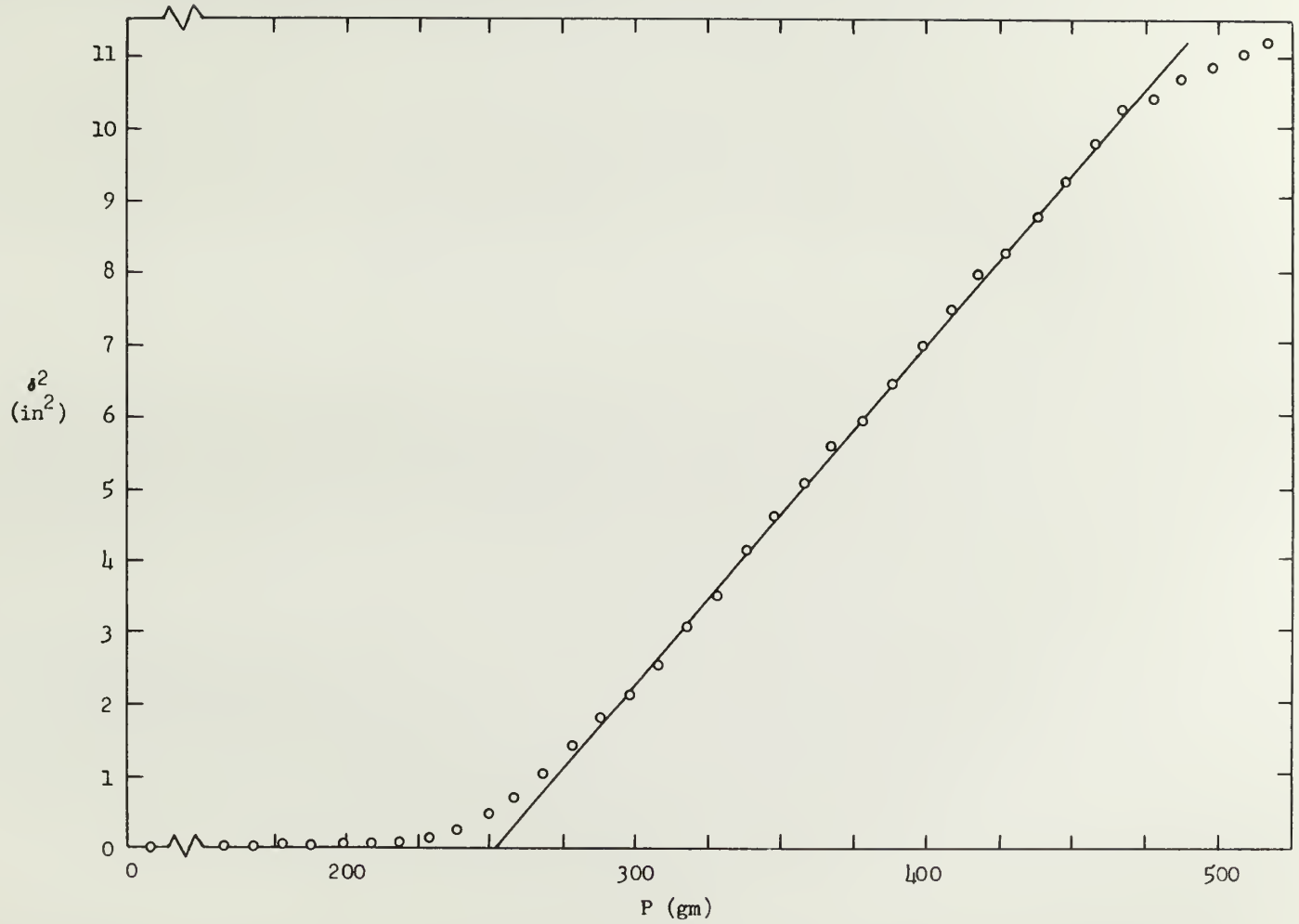

Fig. 11c. Large Deflection Plot for Spring Steel Beam